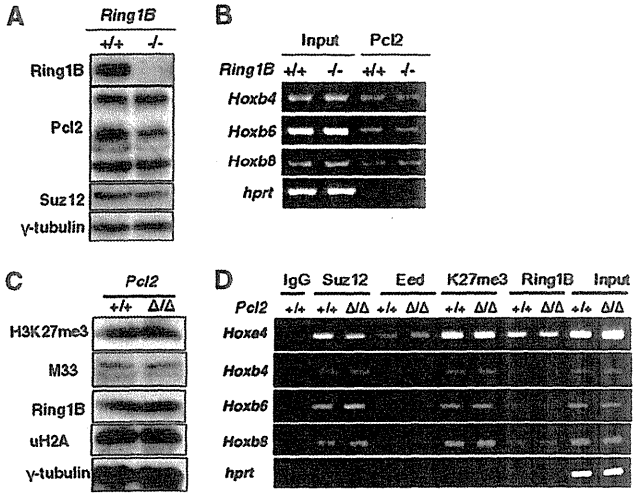

FIG. 4. The expression and target binding of Ring1B and Pcl2 are regulated in a mutually independent manner in ES cells. (A) Pcl2 and Suz12 are expressed in a Ring1B-independent manner. The expression of Ring1B, Pcl2, and Suz12 in *Ring1B*$^{+/+}$ and *Ring1B*$^{-/-}$ ES cells is shown. γ-Tubulin was used as a dose control. (B) Pcl2 binds to *Hox* promoters in a Ring1B-independent manner. Pcl2 association to the *Hox* promoter regions in *Ring1B*$^{+/+}$ and *Ring1B*$^{-/-}$ ES cells is shown. The *hprt* gene was used as a negative control. (C) Global levels of H3K27 trimethylation (H3K27me3), M33, Ring1B, and H2A monoubiquitinylation (uH2A) were not significantly altered in *Pcl2*$^{\Delta/\Delta}$ ES cells (Δ/Δ) compared to levels in the wild type (+/+). γ-Tubulin was used as a dose control. (D) Binding of Suz12, Eed, H3K27me3, and Ring1B at *Hox* promoter regions was not significantly changed in *Pcl2*$^{\Delta/\Delta}$ ES cells (Δ/Δ). IgG and *hprt* genes were used as negative controls.

teractions between *Pcl2* and *Mel18* mutations synergistically enhanced skeletal abnormalities of the respective mutants and influenced the survival of late-gestation fetuses. To further clarify whether interactions between *Pcl2* and *Mel18* involve PRC1, we extended our genetic studies to Phc2, which is another PRC1 component and is known to physically and genetically interact with Mel18 (28). The *Pcl2*$^{\Delta/\Delta}$; *Phc2*$^{-/-}$ fetuses exhibited skeletal phenotypes and late-gestational lethality very similar to the patterns seen in not only *Pcl2*$^{\Delta/\Delta}$; *Mel18*$^{-/-}$ but also *Mel18*$^{-/-}$; *Phc2*$^{-/-}$ and *Phc1*$^{+/-}$; *Phc2*$^{-/-}$ mutants (Fig. 5C and D). These observations indicate a role for Pcl2 in reinforcing *Hox* repression that is mediated by PRC1. The cooccupancy of *Hox* genes by Pcl2 together with PRC2 and PRC1 suggests that Pcl2 positively regulates PRC2 and PRC1 to repress *Hox* genes during A-P specification of the axis.

***Cdkn2a* activation by Pcl2 in MEFs involves suppression of PRC2.** We went on to examine the functional implication of Pcl2 to mediate Polycomb repression in other cellular contexts. Senescence is a fundamental cellular program that is activated under various forms of stress and acts to prevent further cell proliferation. When a population of cells is propagated in culture, they are exposed to various extrinsic and intrinsic stresses, and the cell population gradually stops dividing. Two definitive tumor suppressor pathways, ARF/MDM2/p53 and p16^{INK4a}/Rb, have been shown to play critical roles in the induction of cellular senescence (59). Central mediators for cellular senescence, p19^{arf} and p16^{Ink4a}, are encoded by the *Cdkn2a* locus, which is known as an essential target of PRC1 (30). PRC1 represses p19^{arf} and p16^{Ink4a} in embryonic fibroblasts (MEFs) and thus protects MEFs to some extent from stress-induced premature senescence. This PRC1-dependent regulation of *Cdkn2a* has also been shown to be active in various stem and progenitor cells.

We first examined the binding of Pcl2 to the *Cdkn2a* locus by ChIP-seq analysis and found considerable Pcl2 deposition together with Ezh2, H3K27me3, and Ring1B in ES cells (Fig. 6A). To test the role of Pcl2 in the regulation of p19^{arf} and p16^{Ink4a} expression, we generated MEFs from *Pcl2*$^{\Delta/\Delta}$ and wild-type littermates and compared progression of cellular senescence by a 3T9 assay (Fig. 6B). To our surprise, growth of *Pcl2*$^{\Delta/\Delta}$ MEFs was similar to that of wild-type MEFs until passage 10, but then the cells failed to stop dividing and continued exponential growth over 50 passages while *Phc2*$^{-/-}$ MEFs prematurely senesced. We further found that *Pcl2*$^{GT/GT}$ MEFs similarly bypassed senescence (Fig. 6C). To confirm that this effect is directly due to Pcl2 loss, we expressed Pcl2 in immortalized *Pcl2*$^{GT/GT}$ MEFs by retroviral transduction. Ectopic expression of Pcl2 indeed induced cellular senescence in immortalized *Pcl2*$^{GT/GT}$ MEFs (Fig. 6D). Consistent with these phenotypes, *Pcl2*$^{\Delta/\Delta}$ MEFs did not exhibit morphological features characteristic of senescent MEFs at passage 12 (Fig. 6E). We went on to investigate the expression of p19^{arf} and p16^{Ink4a} in *Pcl2*$^{\Delta/\Delta}$ MEFs and observed their strong repression at passage 10 (Fig. 6F). This was accompanied by a reduction of *p19*^{arf} and *p16*^{Ink4a} transcripts (Fig. 6G). Therefore, these results suggest that *Pcl2*$^{\Delta/\Delta}$ MEFs fail to undergo cellular senescence.

We next tested the functional involvement of *Cdkn2a* repression in terminating cellular senescence. To this end, we expressed p19^{arf} or p16^{Ink4a} in *Pcl2*$^{\Delta/\Delta}$ MEFs by retroviral transduction. Proliferation of *Pcl2*$^{\Delta/\Delta}$ MEFs was clearly inhibited by either p19^{arf} or p16^{Ink4a} (Fig. 6H), thus suggesting that Pcl2 promotes cellular senescence by activating the expression of *Cdkn2a* genes in MEFs. To further test this hypothesis, we overexpressed Pcl2 in MEFs. We generated a transgenic mouse, in which expression of the 67-kDa isoform of Pcl2 could be induced by tamoxifen-dependent activation of ERT2-Cre (Fig. 7A). Proliferation of these MEFs was impaired by tamoxifen treatment (Fig. 7B), and the mitotic arrest was accompanied by activation of p19^{arf} (Fig. 7C). Therefore, we showed that Pcl2 plays a role as an activator of *Cdkn2a* expression, whereas PRC1 functions as a repressor in MEFs.

We went on to test whether this positive effect of Pcl2 on *Cdkn2a* transcription involved regulation of the catalytic activity of PRC2. We performed ChIP analysis to test H3K27me3 occupancy at the *p16*^{Ink4a} promoter region in *Pcl2*$^{GT/GT}$ MEFs (Fig. 8A and B). Local H3K27me3 levels at this promoter were significantly increased in *Pcl2*$^{GT/GT}$ MEFs compared to levels the wild-type cells. Consistent with the transcriptional status of *p16*^{Ink4a}, we also found decrease H3K4me3 in *Pcl2*$^{GT/GT}$ MEFs. Pcl2 therefore activates *Cdkn2a* expression, presumably by suppressing local catalytic activity of PRC2.

In addition, we examined whether Pcl2-dependent regulation of *Cdkn2a* involves PRC1. We generated *Pcl2* and *Phc2* double mutant MEFs and compared the level of cellular senescence to that observed in the single mutants (Fig. 6B). Notably, *Pcl2*$^{\Delta/\Delta}$; *Phc2*$^{-/-}$ MEFs, as well as *Phc2*$^{-/-}$ MEFs,

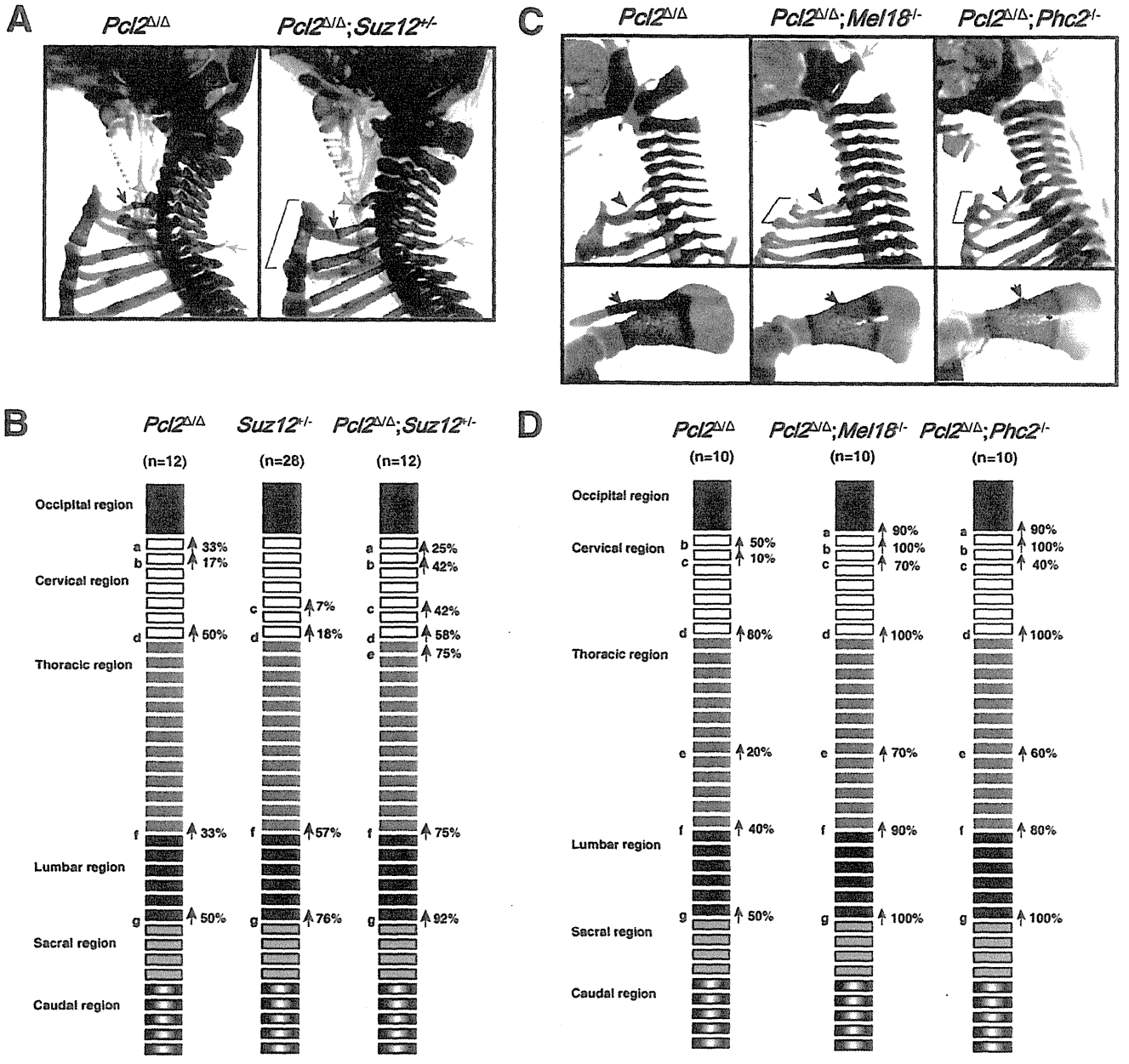

FIG. 5. Synergistic activity of Pcl2 with PRC2 and PRC1 components during A-P specification of the axis. (A) Lateral views of the upper part of the vertebral column in *Pcl2*$^{\Delta/\Delta}$ and *Pcl2*$^{\Delta/\Delta}$; *Suz12*$^{+/-}$ newborn mice. Genotypes of *Pcl2* and *Suz12* loci are indicated at the top. Anterior tubercles, ectopic ribs, and prominent spinous processes are indicated by yellow arrowheads, black arrows, and yellow arrows, respectively. A bracket in *Pcl2*$^{\Delta/\Delta}$; *Suz12*$^{+/-}$ indicates the cranially shifted sternum. (B) Schematic representation of the frequency of the axial homeotic transformations in respective mutants. The following parameters, identified by letters on the figure, were scored, and the frequency of each alteration is indicated: C1 → C2, presence of the odontoid process on the C1 vertebra (a); C2 → C3, lack of the odontoid process from the C2 vertebra (b); C5 → C6, appearance of the anterior tubercle of the transverse process on the C5 (c); C7 → T1, appearance of cervical ribs on C7 (d); T1 → T2, prominent spinous process on T1 (e); T13 → L1, loss of the rib on 20th vertebra (f); L5 or L6 → S1, formation of the sacroiliac joint in the 25th or 26th vertebra (g). (C) Skeletal alterations seen in *Pcl2*$^{\Delta/\Delta}$, *Pcl2*$^{\Delta/\Delta}$; *Mel18*$^{-/-}$, and *Pcl2*$^{\Delta/\Delta}$; *Phc2*$^{-/-}$ mice. Only the mutant *Pcl2*, *Mel18*, and *Phc2* alleles are depicted. (Upper panels show lateral views of the upper part of the vertebral column. Arrowheads indicate ectopic ribs associated with C7. For *Pcl2*$^{\Delta/\Delta}$; *Mel18*$^{-/-}$ and *Pcl2*$^{\Delta/\Delta}$; *Phc2*$^{-/-}$ mice, yellow arrows and brackets indicate ectopic arches of the occipital bone and cranially shifted sternum, respectively. Lower panels show overviews of the scapula. Acromion are indicated by arrows, which are rudimentary in the compound mutants. Holes (asterisks) were generated in the center of blades in *Pcl2*$^{\Delta/\Delta}$; *Mel18*$^{-/-}$ and *Pcl2*$^{\Delta/\Delta}$; *Phc2*$^{-/-}$ mice. (D) Schematic representation of the frequency of the axial homeotic transformations in respective mutants. The following parameters, identified by letters on the figure, were scored, and the frequency of each alteration is indicated: supraoccipital bone → C1, appearance of ectopic bones seen in the craniodorsal region of the C1 vertebra or ectopic arch of the occipital bones (a); C1 → C2, presence of the odontoid process on the C1 vertebra (b); C2 → C3, lack of the odontoid process from the C2 vertebra (c); C7 → T1, appearance of cervical ribs on C7 (d); T7 → T8, dissociation of seventh rib from the sternum (e); T13 → L1, loss of the rib on the 20th vertebra (f); L5 or L6 → S1, formation of the sacroiliac joint in 25th or 26th vertebra (g).

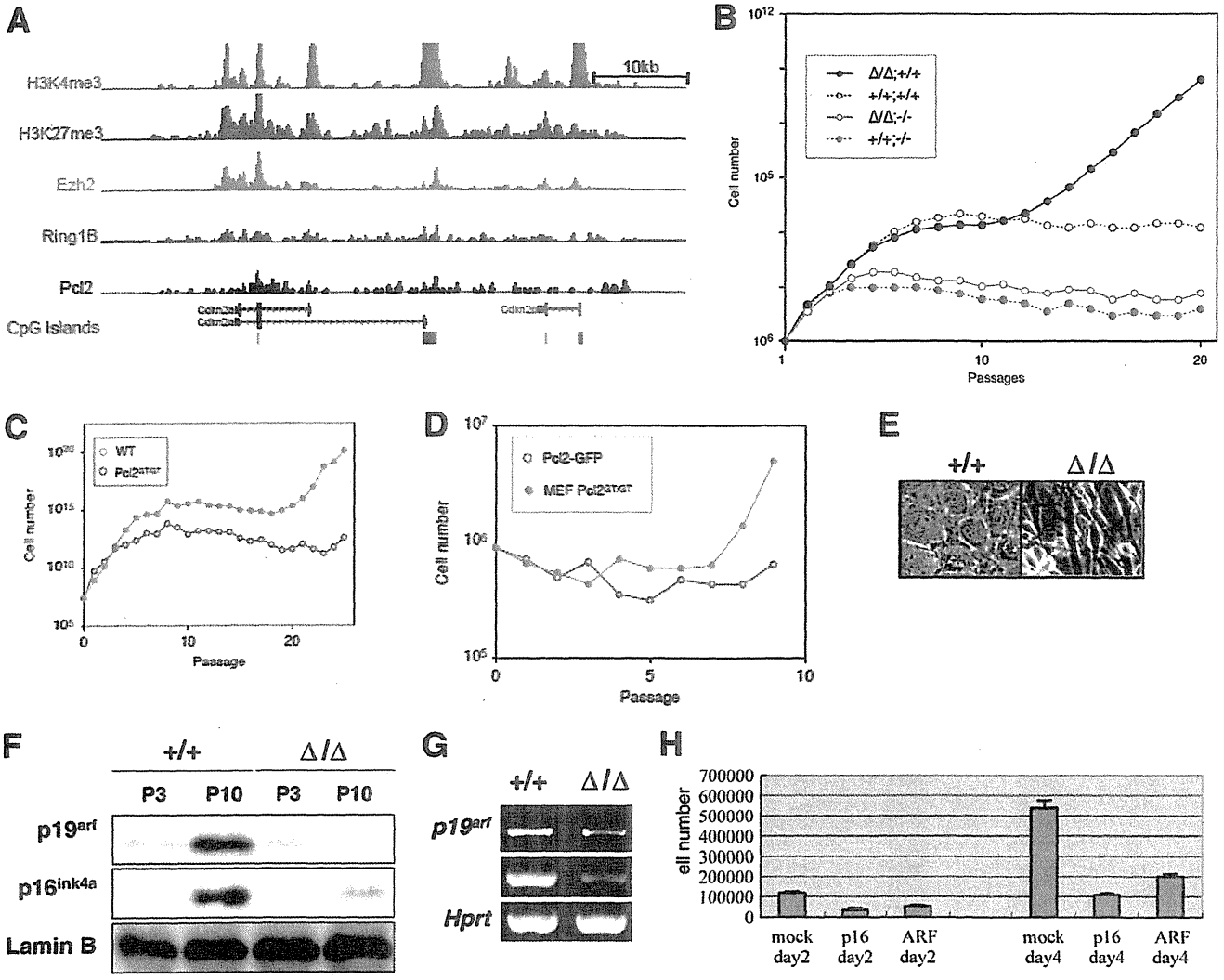

FIG. 6. The role of Pcl2 in replicative senescence. (A) ChIP-seq binding patterns at *Cdkn2a* and *Cdkn2b* loci are shown for H3K4me3, H3K27me3, Ezh2, Ring1B, and Pcl2 in ES cells. CpG islands are shown as green bars (below) (B) Termination of replicative senescence in $Pcl2^{\Delta/\Delta}$ MEFs as revealed by a modified 3T9 assay. Levels of replicative senescence were compared among the wild-type (+/+; +/+), $Pcl2^{\Delta/\Delta}$ (Δ/Δ; +/+), $Phc2^{-/-}$ (+/+; −/−) and $Pcl2^{\Delta/\Delta}$; $Phc2^{-/-}$ (Δ/Δ; −/−) cells. (C) The role of Pcl2 in replicative senescence. Termination of replicative senescence in $Pcl2^{GT/GT}$ MEFs as revealed by a modified 3T9 assay. Levels of replicative senescence were compared between the wild-type (+/+; +/+) and $Pcl2^{GT/GT}$ MEFs. (D) Overexpression of Pcl2 induced senescence in $Pcl2^{GT/GT}$ MEFs. (E) Morphology of wild-type (+/+) and $Pcl2^{\Delta/\Delta}$ (Δ/Δ) MEFs at passage 12. Light microscopic views are shown. (F) Decreased expression of $p19^{arf}$ and $p16^{ink4a}$ in $Pcl2^{\Delta/\Delta}$ (Δ/Δ) MEFs at passage 10 in comparison with that of the wild type (+/+). The expression of lamin B was examined as a dose control. (G) Quantitative analysis of $p19^{arf}$ and $p16^{ink4a}$ transcripts in $Pcl2^{\Delta/\Delta}$ (Δ/Δ) MEFs at passage 10. Note the concomitant reduction of these transcripts in $Pcl2^{\Delta/\Delta}$ MEFs in comparison with wild type (+/+). (H) *Cdkn2a* repression is involved in inhibiting cellular senescence in $Pcl2^{\Delta/\Delta}$ MEFs. Overexpression of either $p19^{arf}$ or $p16^{Ink4a}$ in $Pcl2^{\Delta/\Delta}$ MEFs considerably inhibited their proliferation. The total cells were counted on day 2 and day 4 after retroviral transduction.

stopped replicating at passage 5. Therefore, the *Pcl2*-deficient phenotype was strongly suppressed by loss of *Phc2*, which implies that Pcl2 functions require PRC1 in regulation of cellular senescence. Consistently, we found a considerable quantity of Ring1B retained at the $p16^{Ink4a}$ promoter in $Pcl2^{GT/GT}$ MEFs although its local level was significantly decreased compared to that of the wild type (Fig. 8A and B). Pcl2 thus profoundly modulates functional engagement of PRC2 and PRC1 to maintain proper expression of *Cdkn2a* under replicative stress.

DISCUSSION

In this study, we have investigated the role of Pcl2 at two canonical Polycomb targets, the *Hox* cluster and *Cdkn2a* genes, by combining genetic and biochemical approaches. We have first identified Pcl2 gene products and their functions in *Hox* repression during A-P specification by using two mutant alleles. The expression of Pcl2 and its binding to *Hox* genes were shown to depend on its physical association with PRC2. Interactions of mutant *Pcl2* with *Suz12* indicated the requirement of

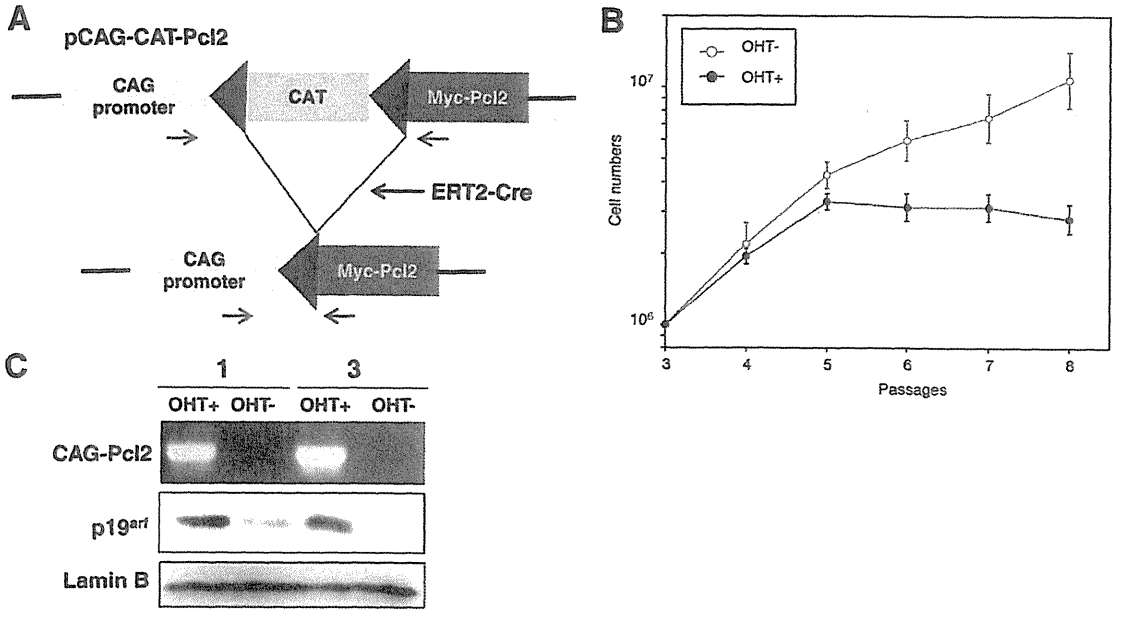

FIG. 7. Pcl2 regulates cellular senescence through *Cdkn2a*. (A) Schematic representation of the transgene to overexpress Myc-tagged Pcl2 in a Cre recombinase-dependent manner. Briefly, the *lacZ* gene in CAG-CAT-Z (4) was replaced by Myc-tagged Pcl2. Pcl2 expression is therefore induced by deletion of chloramphenicol acetyltransferase (CAT) gene cassette placed between two *loxP* sites (shown by arrows) by Cre recombinase. A transgenic line harboring this inducible construct was bred with another transgenic line expressing ERT2-Cre to generate MEFs in which Pcl2 could be expressed upon 4-hydroxytamoxifen ([OHT] 0.5 μM) treatment. The location of primers used to assess deletion of the CAT gene cassette is shown. (B) Impact of Myc-tagged Pcl2 on replicative senescence as revealed by a modified 3T9 assay. Double transgenic MEFs were treated by 0.5 μM tamoxifen at passage 3 (OHT+), and growth rate was examined after the treatment by using untreated MEFs as a control (OHT−). Overexpression of Pcl2 (OHT+) clearly induced premature proliferation arrest. (C) Induction of $p19^{arf}$ expression upon deletion of the CAT gene in two different MEF lines harboring double transgenes. The top panel is an assessment of tamoxifen-induced recombination of the transgene, the middle shows results of Western blotting for $p19^{arf}$ expression, and the bottom shows results of Western blotting for lamin B expression as dose controls.

Pcl2 for PRC2 to exert its functions in *Hox* repression. Therefore, Pcl2 is a functional component of PRC2. It is also noteworthy, however, that the *Pcl2* mutation affects PRC1-mediated repression of *Hox* genes as manifested by genetic interactions between *Pcl2* and *Mel18* or *Phc2* although local depositions of H3K27me3 or Ring1B were not significantly altered in the *Pcl2* mutants. Although the detailed underlying mechanisms are as yet unclear, our results strongly indicate that Pcl2 cooperates with both PRC2 and PRC1 to regulate the expression of *Hox* cluster genes during axial development (Fig. 8C). In contrast, Pcl2 activates the expression of *Cdkn2a* genes once primary fibroblasts become predisposed to stress-induced senescence (Fig. 8C). In this case, Pcl2 could primarily act by suppressing the local catalytic activity of PRC2, which may in turn enable bypassing of PRC1-mediated repression. Taken together, these results show that Pcl2 is required to modify the functional engagement of PRC2 and PRC1 complexes, presumably by sensing cellular circumstances. However, we could not unequivocally exclude the possibility that Pcl2 might have functions independent of PRC2 in regulation of cellular senescence.

Molecular mechanisms that link Pcl2 to such cellular circumstances remain as yet unknown. One intriguing possibility is that Pcl2 might recognize local chromatin cues by its Tudor domain and/or PHD fingers. By using the $Pcl2^{\Delta}$ allele, we have shown a requirement for the 67- and 55-kDa isoforms of Pcl2 to mediate *Hox* repression in developing embryos and *Cdkn2a* activation in MEFs. Based on other recent studies, both Tudor and PHD finger domains have emerged as binding modules for methylated histone tails (7, 26, 34). Particularly, the PHD fingers of Pcl2 are predicted to recognize unmethylated or trimethylated histone H3K4 based on their respective primary structures (42, 52, 60, 65). Polycomb target genes, including *Hox* genes, are known to be bivalently marked by H3K27me3 and H3K4me3 in several cell types. Pcl2 may contribute to the *Hox* regulation via its recognition of the methylation status of H3K4 in developing embryos. In addition to detection of the methylation status of histone tails, Tudor and PHD finger domains have also been shown to contribute to recognition of RNA and phosphatidylinositols, respectively (7, 22, 26). We thus postulate that Pcl2 might use a combination of the Tudor domain and PHD fingers to discern chromatin circumstances and affect local activity of PRC2 via physical interaction. Identification of ligands for the Pcl2 Tudor domain and PHD fingers will be necessary to fully clarify this issue.

It is well known that the expression of *Hox* genes continues to be dynamically regulated in developing tissues after the initial establishment of their early expression domains (16). This implies that Polycomb-dependent *Hox* repression is plastic with the potential to be reactivated, presumably by various differentiation cues. In line with this, PRC1 has been shown to be linked to inductive signals mediating cellular differentiation, survival, and/or proliferation in cerebellar progenitors and ES cells (18, 39). Moreover, recent studies demonstrate that dy-

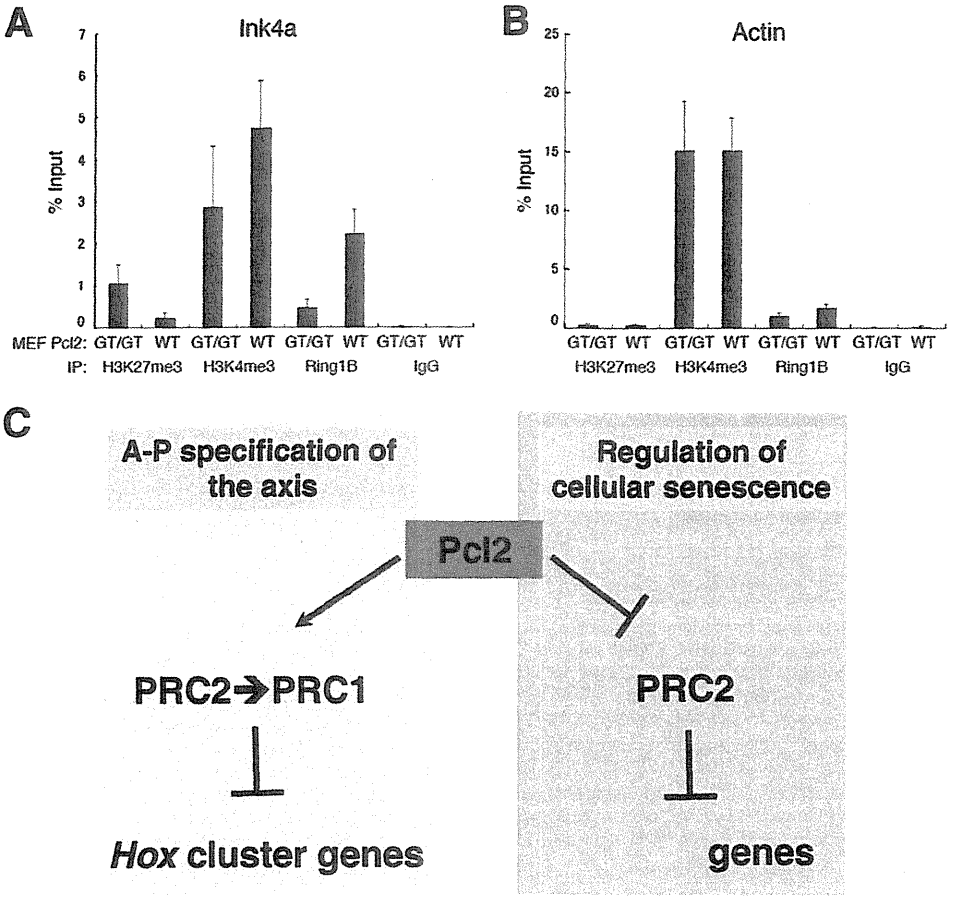

FIG. 8. The role of Pcl2 for PRC2 and PRC1. (A and B) Enrichment of H3K27me3, H3K4me3, and Ring1B at the $p16^{Ink4a}$ promoter region was determined by ChIP and site-specific real-time PCR. The β-actin promoter was used as a control. (C) A model for Pcl2 functions during A-P specification of the axis and stress-induced cellular senescence. In developing embryos, Pcl2 is a functional component of PRC2 and also functionally cooperates with PRC1 to mediate repression of *Hox* cluster genes. Upon replicative stress, Pcl2 activates *Cdkn2a* expression and suppresses cellular senescence, likely by suppressing the catalytic activity of PRC2 at the *Cdkn2a* locus.

namic regulation of Polycomb activity orchestrated by the Jumonji (or Jarid2) protein included in PRC2 balances self-renewal and differentiation of ES cells (58). In this regard, it is worthy of note that Pcl2 is copurified with Jumonji (41). Pcl2, in collaboration with proteins such as Jumonji, could act as a module that mediates such plasticity of Polycomb repression by discerning chromatin circumstances induced by differentiation cues.

ACKNOWLEDGMENT

This project was in part supported by Genome Network Project from the Ministry of Education, Culture, Sports, Science and Technology of the Japanese Government (H.K.).

REFERENCES

1. **Akasaka, T., M. Kanno, R. Balling, M. A. Mieza, M. Taniguchi, and H. Koseki.** 1996. A role for mel-18, a Polycomb group-related vertebrate gene, during the anteroposterior specification of the axial skeleton. Development **122**:1513–1522.
2. **Akasaka, T., M. van Lohuizen, N. van der Lugt, Y. Mizutani-Koseki, M. Kanno, M. Taniguchi, M. Vidal, M. Alkema, A. Berns, and H. Koseki.** 2001. Mice doubly deficient for the Polycomb group genes Mel18 and Bmi1 reveal synergy and requirement for maintenance but not initiation of Hox gene expression. Development **128**:1587–1597.
3. **Altschul, S. F., W. Gish, W. Miller, E. W. Myers, and D. J. Lipman.** 1990. Basic local alignment search tool. J. Mol. Biol. **215**:403–410.
4. **Araki, K., M. Araki, J. Miyazaki, and P. Vassalli.** 1995. Site-specific recombination of a transgene in fertilized eggs by transient expression of Cre recombinase. Proc. Natl. Acad. Sci. U. S. A. **92**:160–164.
5. **Atsuta, T., S. Fujimura, H. Moriya, M. Vidal, T. Akasaka, and H. Koseki.** 2001. Production of monoclonal antibodies against mammalian Ring1B proteins. Hybridoma **20**:43–46.
6. **Bel, S., N. Core, M. Djabali, K. Kieboom, N. Van der Lugt, M. J. Alkema, and M. Van Lohuizen.** 1998. Genetic interactions and dosage effects of Polycomb group genes in mice. Development **125**:3543–3551.
7. **Bernstein, E., and C. D. Allis.** 2005. RNA meets chromatin. Genes Dev. **19**:1635–1655.
8. **Boyer, L. A., K. Plath, J. Zeitlinger, T. Brambrink, L. A. Medeiros, T. I. Lee, S. S. Levine, M. Wernig, A. Tajonar, M. K. Ray, G. W. Bell, A. P. Otte, M. Vidal, D. K. Gifford, R. A. Young, and R. Jaenisch.** 2006. Polycomb complexes repress developmental regulators in murine embryonic stem cells. Nature **441**:349–353.
9. **Cao, R., Y. Tsukada, and Y. Zhang.** 2005. Role of Bmi-1 and Ring1A in H2A ubiquitylation and Hox gene silencing. Mol. Cell **20**:845–854.
10. **Cao, R., H. Wang, J. He, H. Erdjument-Bromage, P. Tempst, and Y. Zhang.** 2008. Role of hPHF1 in H3K27 methylation and Hox gene silencing. Mol. Cell. Biol. **28**:1862–1872.
11. **Cao, R., L. Wang, H. Wang, L. Xia, H. Erdjument-Bromage, P. Tempst, R. S. Jones, and Y. Zhang.** 2002. Role of histone H3 lysine 27 methylation in Polycomb-group silencing. Science **298**:1039–1043.
12. **Coulson, M., S. Robert, H. J. Eyre, and R. Saint.** 1998. The identification and localization of a human gene with sequence similarity to Polycomblike of *Drosophila melanogaster*. Genomics **48**:381–383.
13. **Czermin, B., R. Melfi, D. McCabe, V. Seitz, A. Imhof, and V. Pirrotta.** 2002. *Drosophila* enhancer of Zeste/ESC complexes have a histone H3 methyl-

transferase activity that marks chromosomal Polycomb sites. Cell **111**:185–196.
14. **de Napoles, M., J. E. Mermoud, R. Wakao, Y. A. Tang, M. Endoh, R. Appanah, T. B. Nesterova, J. Silva, A. P. Otte, M. Vidal, H. Koseki, and N. Brockdorff.** 2004. Polycomb group proteins Ring1A/B link ubiquitylation of histone H2A to heritable gene silencing and X inactivation. Dev. Cell **7**:663–676.
15. **Dignam, J. D., R. M. Lebovitz, and R. G. Roeder.** 1983. Accurate transcription initiation by RNA polymerase II in a soluble extract from isolated mammalian nuclei. Nucleic Acids Res. **11**:1475–1489.
16. **Duboule, D.** 1995. Vertebrate Hox genes and proliferation: an alternative pathway to homeosis? Curr. Opin. Genet. Dev. **5**:525–528.
17. **Duncan, I. M.** 1982. Polycomblike: a gene that appears to be required for the normal expression of the bithorax and antennapedia gene complexes of *Drosophila melanogaster*. Genetics **102**:49–70.
18. **Endoh, M., T. A. Endo, T. Endoh, Y. Fujimura, O. Ohara, T. Toyoda, A. P. Otte, M. Okano, N. Brockdorff, M. Vidal, and H. Koseki.** 2008. Polycomb group proteins Ring1A/B are functionally linked to the core transcriptional regulatory circuitry to maintain ES cell identity. Development **135**:1513–1524.
19. **Eskeland, R., M. Leeb, G. R. Grimes, C. Kress, S. Boyle, D. Sproul, N. Gilbert, Y. Fan, A. I. Skoultchi, A. Wutz, and W. A. Bickmore.** 2010. Ring1B compacts chromatin structure and represses gene expression independent of histone ubiquitination. Mol. Cell **38**:452–464.
20. **Francis, N. J., A. J. Saurin, Z. Shao, and R. E. Kingston.** 2001. Reconstitution of a functional core polycomb repressive complex. Mol. Cell **8**:545–556.
21. **Fujimura, Y., K. Isono, M. Vidal, M. Endoh, H. Kajita, Y. Mizutani-Koseki, Y. Takihara, M. van Lohuizen, A. Otte, T. Jenuwein, J. Deschamps, and H. Koseki.** 2006. Distinct roles of Polycomb group gene products in transcriptionally repressed and active domains of Hoxb8. Development **133**:2371–2381.
22. **Gozani, O., P. Karuman, D. R. Jones, D. Ivanov, J. Cha, A. A. Lugovskoy, C. L. Baird, H. Zhu, S. J. Field, S. L. Lessnick, J. Villasenor, B. Mehrotra, J. Chen, V. R. Rao, J. S. Brugge, C. G. Ferguson, B. Payrastre, D. G. Myszka, L. C. Cantley, G. Wagner, N. Divecha, G. D. Prestwich, and J. Yuan.** 2003. The PHD finger of the chromatin-associated protein ING2 functions as a nuclear phosphoinositide receptor. Cell **114**:99–111.
23. **Hamer, K. M., R. G. Sewalt, J. L. den Blaauwen, T. Hendrix, D. P. Satijn, and A. P. Otte.** 2002. A panel of monoclonal antibodies against human polycomb group proteins. Hybrid. Hybridomics **21**:245–252.
24. **Hansen, J., T. Floss, P. Van Sloun, E. M. Fuchtbauer, F. Vauti, H. H. Arnold, F. Schnutgen, W. Wurst, H. von Melchner, and P. Ruiz.** 2003. A large-scale, gene-driven mutagenesis approach for the functional analysis of the mouse genome. Proc. Natl. Acad. Sci. U. S. A. **100**:9918–9922.
25. **Hong, Z., J. Jiang, L. Lan, S. Nakajima, S. Kanno, H. Koseki, and A. Yasui.** 2008. A polycomb group protein, PHF1, is involved in the response to DNA double-strand breaks in human cell. Nucleic Acids Res. **36**:2939–2947.
26. **Huyen, Y., O. Zgheib, R. A. Ditullio, Jr., V. G. Gorgoulis, P. Zacharatos, T. J. Petty, E. A. Sheston, H. S. Mellert, E. S. Stavridi, and T. D. Halazonetis.** 2004. Methylated lysine 79 of histone H3 targets 53BP1 to DNA double-strand breaks. Nature **432**:406–411.
27. **Inouye, C., P. Remondelli, M. Karin, and S. Elledge.** 1994. Isolation of a cDNA encoding a metal response element binding protein using a novel expression cloning procedure: the one hybrid system. DNA Cell Biol. **13**: 731–742.
28. **Isono, K., Y. Fujimura, J. Shinga, M. Yamaki, J. O. Wang, Y. Takihara, Y. Murahashi, Y. Takada, Y. Mizutani-Koseki, and H. Koseki.** 2005. Mammalian polyhomeotic homologues Phc2 and Phc1 act in synergy to mediate polycomb repression of *Hox* genes. Mol. Cell. Biol. **25**:6694–6706.
29. **Isono, K., Y. Mizutani-Koseki, T. Komori, M. S. Schmidt-Zachmann, and H. Koseki.** 2005. Mammalian polycomb-mediated repression of Hox genes requires the essential spliceosomal protein Sf3b1. Genes Dev. **19**:536–541.
30. **Jacobs, J. J., K. Kieboom, S. Marino, R. A. DePinho, and M. van Lohuizen.** 1999. The oncogene and Polycomb-group gene *bmi-1* regulates cell proliferation and senescence through the *ink4a* locus. Nature **397**:164–168.
31. **Kamijo, T., F. Zindy, M. F. Roussel, D. E. Quelle, J. R. Downing, R. A. Ashmun, G. Grosveld, and C. J. Sherr.** 1997. Tumor suppression at the mouse INK4a locus mediated by the alternative reading frame product p19ARF. Cell **91**:649–659.
32. **Kawakami, S., K. Mitsunaga, Y. Y. Kikuti, A. Ando, H. Inoko, K. Yamamura, and K. Abe.** 1998. Tctex3, related to *Drosophila* polycomblike, is expressed in male germ cells and mapped to the mouse t-complex. Mamm. Genome **9**:874–880.
33. **Kennison, J. A., and J. W. Tamkun.** 1988. Dosage-dependent modifiers of polycomb and antennapedia mutations in *Drosophila*. Proc. Natl. Acad. Sci. U. S. A. **85**:8136–8140.
34. **Kim, J., J. Daniel, A. Espejo, A. Lake, M. Krishna, L. Xia, Y. Zhang, and M. T. Bedford.** 2006. Tudor, MBT and chromo domains gauge the degree of lysine methylation. EMBO Rep. **7**:397–403.
35. **King, I. F., N. J. Francis, and R. E. Kingston.** 2002. Native and recombinant Polycomb group complexes establish a selective block to template accessibility to repress transcription in vitro. Mol. Cell. Biol. **22**:7919–7928.
36. **Kitaguchi, T., K. Nakata, T. Nagai, J. Aruga, and K. Mikoshiba.** 2001. *Xenopus* Polycomblike 2 (XPcl2) controls anterior to posterior patterning of the neural tissue. Dev. Genes Evol. **211**:309–314.
37. **Ku, M., R. P. Koche, E. Rheinbay, E. M. Mendenhall, M. Endoh, T. S. Mikkelsen, A. Presser, C. Nusbaum, X. Xie, A. S. Chi, M. Adli, S. Kasif, L. M. Ptaszek, C. A. Cowan, E. S. Lander, H. Koseki, and B. E. Bernstein.** 2008. Genomewide analysis of PRC1 and PRC2 occupancy identifies two classes of bivalent domains. PLoS Genet. **4**:e1000242.
38. **Lee, T. I., R. G. Jenner, L. A. Boyer, M. G. Guenther, S. S. Levine, R. M. Kumar, B. Chevalier, S. E. Johnstone, M. F. Cole, K. Isono, H. Koseki, T. Fuchikami, K. Abe, H. L. Murray, J. P. Zucker, B. Yuan, G. W. Bell, E. Herbolsheimer, N. M. Hannett, K. Sun, D. T. Odom, A. P. Otte, T. L. Volkert, D. P. Bartel, D. A. Melton, D. K. Gifford, R. Jaenisch, and R. A. Young.** 2006. Control of developmental regulators by Polycomb in human embryonic stem cells. Cell **125**:301–313.
39. **Leung, C., M. Lingbeek, O. Shakhova, J. Liu, E. Tanger, P. Saremaslani, M. Van Lohuizen, and S. Marino.** 2004. Bmi1 is essential for cerebellar development and is overexpressed in human medulloblastomas. Nature **428**:337–341.
40. **Levine, S. S., A. Weiss, H. Erdjument-Bromage, Z. Shao, P. Tempst, and R. E. Kingston.** 2002. The core of the Polycomb repressive complex is compositionally and functionally conserved in flies and humans. Mol. Cell. Biol. **22**:6070–6078.
41. **Li, G., R. Margueron, M. Ku, P. Chambon, B. E. Bernstein, and D. Reinberg.** 2010. Jarid2 and PRC2, partners in regulating gene expression. Genes Dev. **24**:368–380.
42. **Li, H., S. Ilin, W. Wang, E. M. Duncan, J. Wysocka, C. D. Allis, and D. J. Patel.** 2006. Molecular basis for site-specific read-out of histone H3K4me3 by the BPTF PHD finger of NURF. Nature **442**:91–95.
43. **Lonie, A., R. D'Andrea, R. Paro, and R. Saint.** 1994. Molecular characterisation of the Polycomblike gene of *Drosophila melanogaster*, a trans-acting negative regulator of homeotic gene expression. Development **120**:2629–2636.
44. **Mikkelsen, T. S., M. Ku, D. B. Jaffe, B. Issac, E. Lieberman, G. Giannoukos, P. Alvarez, W. Brockman, T. K. Kim, R. P. Koche, W. Lee, E. Mendenhall, A. O'Donovan, A. Presser, C. Russ, X. Xie, A. Meissner, M. Wernig, R. Jaenisch, C. Nusbaum, E. S. Lander, and B. E. Bernstein.** 2007. Genome-wide maps of chromatin state in pluripotent and lineage-committed cells. Nature **448**:553–560.
45. **Mortazavi, A., B. A. Williams, K. McCue, L. Schaeffer, and B. Wold.** 2008. Mapping and quantifying mammalian transcriptomes by RNA-Seq. Nat. Methods **5**:621–628.
46. **Muller, J., C. M. Hart, N. J. Francis, M. L. Vargas, A. Sengupta, B. Wild, E. L. Miller, M. B. O'Connor, R. E. Kingston, and J. A. Simon.** 2002. Histone methyltransferase activity of a *Drosophila* Polycomb group repressor complex. Cell **111**:197–208.
47. **Nekrasov, M., T. Klymenko, S. Fraterman, B. Papp, K. Oktaba, T. Kocher, A. Cohen, H. G. Stunnenberg, M. Wilm, and J. Muller.** 2007. Pcl-PRC2 is needed to generate high levels of H3-K27 trimethylation at Polycomb target genes. EMBO J. **26**:4078–4088.
48. **O'Carroll, D., S. Erhardt, M. Pagani, S. C. Barton, M. A. Surani, and T. Jenuwein.** 2001. The *Polycomb*-group gene *Ezh2* is required for early mouse development. Mol. Cell. Biol. **21**:4330–4336.
49. **O'Connell, S., L. Wang, S. Robert, C. A. Jones, R. Saint, and R. S. Jones.** 2001. Polycomblike PHD fingers mediate conserved interaction with enhancer of zeste protein. J. Biol. Chem. **276**:43065–43073.
50. **Paro, R.** 1995. Propagating memory of transcriptional states. Trends Genet. **11**:295–297.
51. **Pasini, D., A. P. Bracken, M. R. Jensen, E. Lazzerini Denchi, and K. Helin.** 2004. Suz12 is essential for mouse development and for EZH2 histone methyltransferase activity. EMBO J. **23**:4061–4071.
52. **Pena, P. V., F. Davrazou, X. Shi, K. L. Walter, V. V. Verkhusha, O. Gozani, R. Zhao, and T. G. Kutateladze.** 2006. Molecular mechanism of histone H3K4me3 recognition by plant homeodomain of ING2. Nature **442**:100–103.
53. **Pirrotta, V.** 1997. PcG complexes and chromatin silencing. Curr. Opin. Genet. Dev. **7**:249–258.
54. **Sakai, K., and J. Miyazaki.** 1997. A transgenic mouse line that retains Cre recombinase activity in mature oocytes irrespective of the *cre* transgene transmission. Biochem. Biophys. Res. Commun. **237**:318–324.
55. **Sarma, K., R. Margueron, A. Ivanov, V. Pirrotta, and D. Reinberg.** 2008. Ezh2 requires PHF1 to efficiently catalyze H3 lysine 27 trimethylation in vivo. Mol. Cell. Biol. **28**:2718–2731.
56. **Savla, U., J. Benes, J. Zhang, and R. S. Jones.** 2008. Recruitment of *Drosophila* Polycomb-group proteins by Polycomblike, a component of a novel protein complex in larvae. Development **135**:813–817.
57. **Shao, Z., F. Raible, R. Mollaaghababa, J. R. Guyon, C. T. Wu, W. Bender, and R. E. Kingston.** 1999. Stabilization of chromatin structure by PRC1, a Polycomb complex. Cell **98**:37–46.
58. **Shen, X., W. Kim, Y. Fujiwara, M. D. Simon, Y. Liu, M. R. Mysliwiec, G. C. Yuan, Y. Lee, and S. H. Orkin.** 2009. Jumonji modulates polycomb activity and self-renewal versus differentiation of stem cells. Cell **139**:1303–1314.

59. **Sherr, C. J., and R. A. DePinho.** 2000. Cellular senescence: mitotic clock or culture shock? Cell **102**:407–410.
60. **Shi, X., T. Hong, K. L. Walter, M. Ewalt, E. Michishita, T. Hung, D. Carney, P. Pena, F. Lan, M. R. Kaadige, N. Lacoste, C. Cayrou, F. Davrazou, A. Saha, B. R. Cairns, D. E. Ayer, T. G. Kutateladze, Y. Shi, J. Cote, K. F. Chua, and O. Gozani.** 2006. ING2 PHD domain links histone H3 lysine 4 methylation to active gene repression. Nature **442**:96–99.
61. **Shumacher, A., C. Faust, and T. Magnuson.** 1996. Positional cloning of a global regulator of anterior-posterior patterning in mice. Nature **383**:250–253.
62. **Tie, F., J. Prasad-Sinha, A. Birve, A. Rasmuson-Lestander, and P. J. Harte.** 2003. A 1-megadalton ESC/E(Z) complex from *Drosophila* that contains polycomblike and RPD3. Mol. Cell. Biol. **23**:3352–3362.
63. **Walker, E., W. Y. Chang, J. Hunkapiller, G. Cagney, K. Garcha, J. Torchia, N. J. Krogan, J. F. Reiter, and W. L. Stanford.** 2010. Polycomb-like 2 associates with PRC2 and regulates transcriptional networks during mouse embryonic stem cell self-renewal and differentiation. Cell Stem Cell **6**:153–166.
64. **Wang, H., L. Wang, H. Erdjument-Bromage, M. Vidal, P. Tempst, R. S. Jones, and Y. Zhang.** 2004. Role of histone H2A ubiquitination in Polycomb silencing. Nature **431**:873–878.
65. **Wang, S., F. He, W. Xiong, S. Gu, H. Liu, T. Zhang, X. Yu, and Y. Chen.** 2007. Polycomblike-2-deficient mice exhibit normal left-right asymmetry. Dev. Dyn. **236**:853–861.
66. **Wang, S., X. Yu, T. Zhang, X. Zhang, Z. Zhang, and Y. Chen.** 2004. Chick Pcl2 regulates the left-right asymmetry by repressing Shh expression in Hensen's node. Development **131**:4381–4391.

Cancer Cell
Article

CBX8, a Polycomb Group Protein, Is Essential for MLL-AF9-Induced Leukemogenesis

Jiaying Tan,[1] Morgan Jones,[2] Haruhiko Koseki,[3] Manabu Nakayama,[4] Andrew G. Muntean,[1] Ivan Maillard,[5] and Jay L. Hess[1,*]

[1]Department of Pathology, University of Michigan Medical School, Ann Arbor, MI 48109, USA
[2]Center for Stem Cell Biology, Life Sciences Institute, Graduate Program in Cell and Molecular Biology and MSTP, University of Michigan Medical School, Ann Arbor, MI 48109, USA
[3]Laboratory for Developmental Genetics, RIKEN Research Center for Allergy and Immunology, Yokohama 230-0045, Japan
[4]Laboratory of Human Gene Research, Department of Human Genome Research, Kazusa DNA Research Institute, Chiba 292-0818, Japan
[5]Center for Stem Cell Biology, Life Sciences Institute, Department of Medicine and Department of Cell and Developmental Biology, University of Michigan Medical School, Ann Arbor, MI 48109, USA
*Correspondence: jayhess@umich.edu
DOI 10.1016/j.ccr.2011.09.008

SUMMARY

Chromosomal translocations involving the mixed lineage leukemia (*MLL*) gene lead to the development of acute leukemias. Constitutive *HOX* gene activation by MLL fusion proteins is required for MLL-mediated leukemogenesis; however, the underlying mechanisms remain elusive. Here, we show that chromobox homolog 8 (CBX8), a Polycomb Group protein that interacts with MLL-AF9 and TIP60, is required for MLL-AF9-induced transcriptional activation and leukemogenesis. Conversely, both CBX8 ablation and specific disruption of the CBX8 interaction by point mutations in MLL-AF9 abrogate *HOX* gene upregulation and abolish MLL-AF9 leukemic transformation. Surprisingly, Cbx8-deficient mice are viable and display no apparent hematopoietic defects. Together, our findings demonstrate that CBX8 plays an essential role in MLL-AF9 transcriptional regulation and leukemogenesis.

INTRODUCTION

Mixed lineage leukemia (MLL), a human homolog of the *Drosophila* trithorax group (TrxG) protein, is a histone H3 lysine 4-specific methyltransferase commonly associated with transcriptional activation (Krivtsov and Armstrong, 2007; Nakamura et al., 2002). MLL is essential for both embryonic development and normal hematopoiesis, mainly through transcriptional regulation of the homeobox (*HOX*) gene family and their cofactors (Dou and Hess, 2008). Chromosome translocations at the *MLL* locus that generate oncogenic MLL fusion proteins are one of the major genetic lesions leading to acute leukemias. In total, *MLL* translocations account for up to 80% of infant leukemias and approximately 10% of adult acute leukemias with generally poor prognosis (Aplan, 2006; Muntean et al., 2010). To date, more than 50 different translocation partners have been identified, of which the most common ones are the transcriptional activators AF9, ENL, and AF4 (Krivtsov and Armstrong, 2007; Monroe et al., 2011; Yokoyama et al., 2010).

It is well established that constitutive activation of *HOX* genes, particularly *HOXA9*, is a key feature of MLL pathogenesis; however, the molecular mechanisms governing the aberrant *HOX* gene activation have not been completely deciphered (Sitwala et al., 2008; Yokoyama and Cleary, 2008). Extensive studies have been conducted to explore the functional significance of both the retained MLL portion and the translocation partners of MLL fusion proteins in transcriptional regulation. On the one hand, the amino-terminal portion of MLL has been shown to be required for the localization of MLL fusion proteins, due to its DNA-binding ability (Ayton et al., 2004; Slany et al., 1998) and

Significance

MLL translocations that generate MLL-rearranged oncoproteins are a common cause of human acute leukemias. Although aberrant target gene activation is known as the primary driver of MLL-rearranged leukemogenesis, the underlying mechanisms remain poorly understood. Here, we demonstrate that chromobox homolog 8 (CBX8), a previously characterized transcription repressor, is a crucial cofactor required for MLL-AF9-induced leukemogenesis. Contrary to its role in the polycomb repressive complex 1, CBX8 facilitates the transcriptional activation of MLL-AF9 target genes, possibly through regulating the recruitment of the histone acetyltransferase TIP60. Strikingly, despite its essential role in MLL-AF9 leukemic transformation, CBX8 appears dispensable for normal hematopoiesis. Our findings suggest that disrupting the interaction between CBX8 and MLL-AF9 may be an effective therapeutic strategy in MLL-rearranged leukemias.

the Menin-LEDGF association (Yokoyama and Cleary, 2008). Moreover, we and others have shown that the polymerase-associated factor complex (PAFc), an important component of the basal transcriptional machinery, interacts with this region to facilitate transcriptional activation and leukemic transformation (Milne et al., 2010; Muntean et al., 2010; Tan et al., 2010). On the other hand, the mechanisms by which the major fusion partners contribute to MLL-rearranged leukemogenesis are beginning to be defined (Monroe et al., 2011). It has been reported that a complex of proteins termed ENL-associated proteins (EAPs), or a closely related complex named AEP for AF4 family/ENL family/P-TEFb complex, interacts with the major MLL fusion partners AF9, ENL, and AF4 (Lin et al., 2010; Muntean et al., 2010; Yokoyama et al., 2010). The EAP complex includes not only the common MLL fusion partners but also the histone methyltransferase DOT1L and the P-TEFb complex (consisting of CDK9 and cyclin T1), positively regulating transcription elongation (Krivtsov et al., 2008; Mueller et al., 2007). Meanwhile, other investigators have described an H3K79 methyltransferase complex, DotCom, containing several frequent MLL fusion partners, including AF9, ENL, and AF10, that plays a positive role in leukemogenesis (Mohan et al., 2010b). The components of these complexes partially overlap, suggesting the presence of separate complexes that contribute to MLL-rearranged leukemogenesis (Mohan et al., 2010a; Mueller et al., 2007). Interestingly, chromobox homolog 8 (CBX8), a Polycomb Group (PcG) protein generally associated with transcription repression, is also present in complexes recruited by MLL fusion proteins (Monroe et al., 2011; Mueller et al., 2007). However, the significance of this association has not been defined.

CBX8, also known as HPC3 (*H*uman *P*olycomb *3*), belongs to the CBX protein family (including CBX2, 4, 6, 7, and 8) that is homologs of the *Drosophila* Polycomb (Pc) protein (Kerppola, 2009). CBX8 was originally characterized as a transcriptional repressor, interacting with RING1a/b and associating with BMI1 in the Polycomb repressive complex 1 (PRC1) (Bárdos et al., 2000). A previous study has reported that as a PRC1 component, CBX8 represses the *INK4a/ARF* expression in fibroblasts (Dietrich et al., 2007). Further studies showed that several distinct PRC1 complexes colocalize and regulate *INK4a/ARF* expression, suggesting that the *INK4a/ARF* locus is a general target for PRC1 complexes, rather than a CBX8-specific downstream target (Maertens et al., 2009). Therefore, the exact role of CBX8 in transcriptional regulation remains largely undefined. It has been reported that certain CBX proteins, such as CBX4, can associate with protein complexes other than PRC1, thereby playing a PRC1-independent role in transcriptional regulation (Kerppola, 2009). However, it remains unknown whether CBX8 has a PRC1-independent function and what its biological significance may be.

In the present study we investigated the role of CBX8 in MLL-AF9-induced leukemogenesis and explored the underlying mechanisms in relation to its involvement in PRC1.

RESULTS

CBX8 Specifically Interacts with MLL-AF9 at the C-Terminal Domain (CTD)

Previous studies have reported that the MLL fusion partner AF9 directly interacts with CBX8 through the evolutionarily conserved CTD (Figure 1A) (García-Cuéllar et al., 2001; Hemenway et al., 2001; Monroe et al., 2011). However, whether this interaction is retained in the MLL-AF9 fusion protein has not been defined. To address this question, we transiently coexpressed epitope-tagged MLL-AF9 and CBX8 in human embryonic kidney 293 cells, using a FLAG-tagged "empty" vector as a negative control. Specific interaction between CBX8 and MLL-AF9 was detected by immunoprecipitation (IP) experiments. When using AF9-conjugated agarose beads to pull down the full-length fusion protein, we consistently observed that CBX8 coprecipitated with MLL-AF9 (Figure 1B). To further characterize this interaction, we performed IP experiments in the presence of Benzonase. Using anti-FLAG antibody to pull down FLAG-tagged MLL-AF9, we detected endogenous CBX8 coprecipitating with the fusion protein, indicating that CBX8 interacts with MLL-AF9 in a DNA-independent manner (Figure 1C; see Figure S1A available online). Next, we characterized the critical CBX8 interaction sites on MLL-AF9, by generating 15 point mutants within the CTD through single amino acid substitution. By coimmunoprecipitation (coIP) experiments, we identified two point mutants (T542A and T554A) that specifically disrupt the CBX8 interaction (Figures 1A and 1D). This observation was further supported by reciprocal coIP experiments, using anti-FLAG or anti-Myc antibodies to pull down CBX8 or CxxC-AF9, respectively (Figure 1E; Figure S1B), in which case CxxC-AF9, a previously characterized MLL-AF9 fragment, was used as a surrogate for the full-length fusion protein (Muntean et al., 2010).

Apart from CBX8, AF9 also associates either directly or indirectly with DOT1L, the P-TEFb complex (CDK9 and CYCLINT1) and AF5q31 (Monroe et al., 2011). Therefore, we asked whether the CBX8 interaction is required for interaction with any of these cofactors. To this end, we transiently transfected Myc-tagged CxxC-AF9 (WT or the mutants) in 293 cells and found that the P-TEFb complex (CDK9 and CYCLINT1) and AF5q31 coprecipitated with both the WT CxxC-AF9 fragment and the mutants (Figure 1F). Moreover, the interaction between DOT1L and CxxC-AF9 was also retained in the T542A and T554A mutants, as shown by reciprocal IP experiments using anti-FLAG or anti-HA antibodies to pull down CBX8 or DOT1L, respectively (Figure 1G; Figure S1C). This observation was further confirmed by IP experiments in the context of full-length MLL-AF9 (Figure S1D). Together, our results showed that CBX8 specifically interacts with MLL-AF9 at the CTD, and that disrupting the CBX8 interaction does not affect the interaction with either P-TEFb or DOT1L, both of which are required for MLL-AF9-induced leukemogenesis.

CBX8 Is Essential for Both Initiation and Maintenance of MLL-AF9 Leukemic Transformation

To assess the importance of the CBX8 interaction in MLL-AF9-induced transformation, we first used bone marrow transformation (BMT) assays to examine the transformation ability of the MLL-AF9 mutants (T542A and T554A), which lack the CBX8 interaction. Briefly, Lin- hematopoietic cells derived from primary murine bone marrow (BM) were retrovirally transduced with either WT MLL-AF9 or the mutants, followed by three consecutive rounds of plating (Figure 2A). Despite the comparable expression of the fusion transcripts, as confirmed by real-time

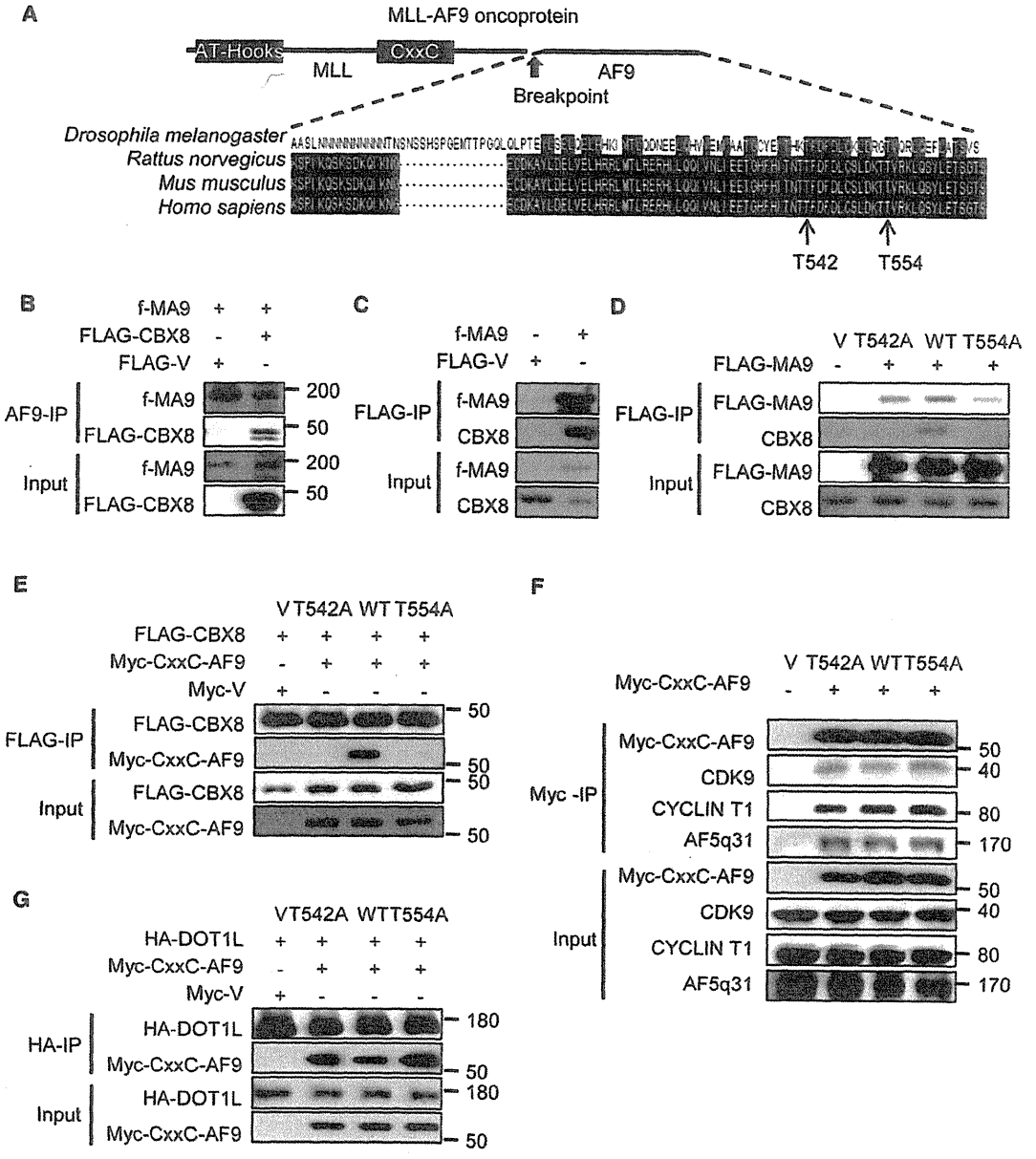

Figure 1. CBX8 Specifically Interacts with MLL-AF9 at the CTD

(A) Schematic of full-length MLL-AF9. The amino acid sequence of the evolutionarily conserved CTD of AF9 is aligned with *Drosophila*, *Rattus norvegicus*, and *Mus musculus* AF9 homologs. Arrows indicate the evolutionarily conserved threonine residues converted to alanine used below.

(B) coIP of FLAG-tagged CBX8 with fMLL-AF9 (f-MA9).

(C) coIP of endogenous CBX8 with f-MA9, after Benzonase treatment.

(D) coIP of endogenous CBX8 with WT FLAG-MA9, but not with the mutants (T542A and T554A).

(E) coIP of FLAG-CBX8 with WT Myc-CxxC-AF9, but not the mutants.

(F) coIP of endogenous CDK9, CYCLIN T1, and AF5q31 with both WT Myc-CxxC-AF9 and the mutants.

(G) coIP of both WT Myc-CxxC-AF9 and the mutants with HA-DOT1L. All of the coIP experiments included an epitope-tagged empty vector (FLAG-V or Myc-V) as a control and were performed in 293 cells. A fraction (3%) of cell lysate was used for input control.

See also Figure S1.

quantitative polymerase chain reaction (RT-qPCR), the T542A and T554A mutations completely abolished myeloid transformation very early on, whereas the WT control potently transformed primary hematopoietic cells, forming a large number of colonies (Figures 2B and 2C). The tertiary colonies formed by WT MLL-AF9-transduced cells displayed a dense, compact morphology, indicative of immortalization. Wright-Giemsa staining shows that these colonies are composed of myeloblasts (Figure 2D).

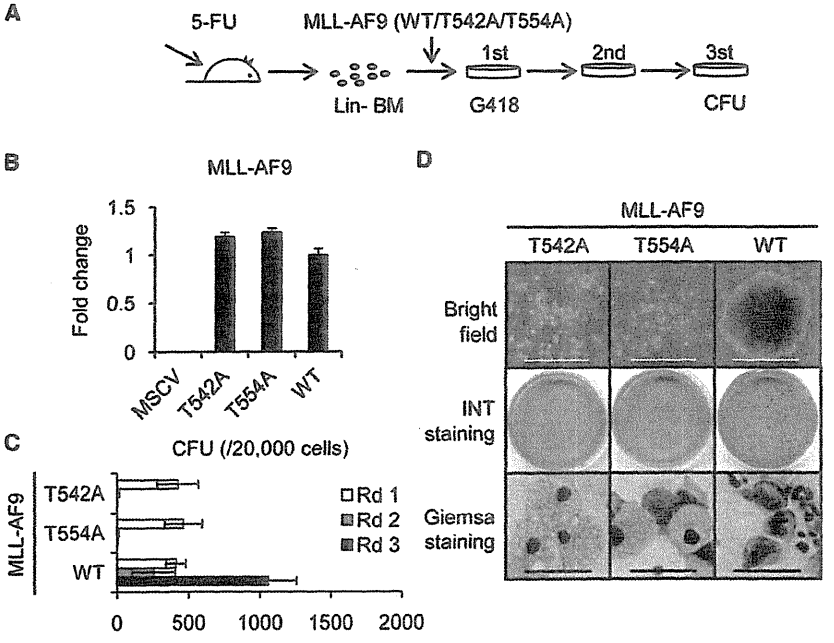

Figure 2. CBX8/MLL-AF9 Interaction Is Essential for MLL-AF9 Leukemic Transformation

(A) Experimental scheme of the BMT assays evaluating the leukemic transformation ability of WT MLL-AF9 and MLL-AF9 mutants (T542A and T554A).

(B) RT-qPCR analysis of the expression levels of WT MLL-AF9 and the mutants in Lin- BM after retroviral transduction.

(C) Colony-forming units (CFU) per 20,000 plated cells in each round of plating in methylcellulose. Error bars represent ± standard deviation (SD) from three independent experiments.

(D) Morphology of representative colonies from primary BM cells transduced with indicated constructs. The first row shows the representative colony morphology in methylcellulose. Scale bars, 500 μm. The second row shows the p-iodonitrotetrazolium violet (INT)-stained colonies after two rounds of plating. Dense red colonies are visible from WT MLL-AF9. The third row shows the Wright-Giemsa-stained cells isolated after two rounds of plating. Scale bars, 50 μm.

See also Figure S2.

In contrast, the MLL-AF9 mutant-transduced cells failed to form colonies in the second round of selection, and they were composed primarily of monocytes and macrophages (Figure 2D). To further confirm that Cbx8 is required for MLL-AF9-induced transformation, we transduced the MLL-AF9-transformed BM cells with either the control shRNA or a shRNA directed against Cbx8 after the third round plating, followed by puromycin selection (Figure S2A). *Cbx8* expression, as measured by RT-qPCR, was effectively downregulated (Figure S2B), whereas the *MLL-AF9* expression level was not significantly affected ($p > 0.05$; Figure S2C). As expected, knockdown of Cbx8 significantly reduced the colony formation ability of MLL-AF9-transduced cells, compared to the control ($p < 0.01$; Figures S2D and S2E). Together, these results suggest that the CBX8/MLL-AF9 interaction is required for MLL-AF9-mediated immortalization.

We then used a conditional *Cbx8* knockout mouse model (generated by H.K.) to further assess the role of Cbx8 in initiation and maintenance of transformation by MLL-fusion proteins in vitro and in vivo (Figure 3A). *Cbx8*$^{f/f}$ mice were bred with Rosa26-*Cre-ERT2* mice to generate *Cbx8* conditional knockout mice. Treatment with 4-hydroxyltamoxifen (4-OHT) induced efficient *Cbx8* excision in primary BM cells from *Cbx8*$^{f/f}$; *Cre*$^{+}$ mice (Figure 3B). To assess the role of Cbx8 in initiation and maintenance of MLL-AF9 leukemic transformation, we induced *Cbx8* excision by 4-OHT treatment, simultaneously with MLL-AF9 transduction or after selecting MLL-AF9-transformed cells by three consecutive rounds of plating, respectively, with BM from *Cbx8*$^{f/f}$; *Cre*$^{-}$ mice serving as a control (Figure 3C). The expression level of MLL-AF9 was not significantly altered by 4-OHT treatment in either of these experimental settings (Figures S3B and S3C). Strikingly, loss of *Cbx8* completely abolished colony formation by MLL-AF9-transduced cells under both conditions (Figures 3D–3F; Figure S3A). In contrast to the colonies formed by *Cbx8*$^{f/f}$; *Cre*$^{+}$ cells with the control treatment and the *Cbx8*$^{f/f}$; *Cre*$^{-}$ control cells with or without 4-OHT treatment, which showed dense morphology and were composed predominantly of myeloblasts (Figure 3G; data not shown), Cbx8-depleted cells failed to form colonies and were composed of monocytes and macrophages (Figure 3G). Together, our results strongly indicate that Cbx8 is essential for both initiation and maintenance of MLL-AF9 leukemic transformation.

Given our findings with the BMT assay, an in vitro surrogate for assessing myeloid transformation ability (Cheung et al., 2007; Lavau et al., 1997; Smith et al., 2011), we then tested the role of Cbx8 in MLL-AF9 leukemogenesis in vivo. The MigR1-MLL-AF9 construct, which expresses both MLL-AF9 and GFP, was used to retrovirally transduce Lin- BM cells derived from the *Cbx8*$^{f/f}$; *Cre*$^{+}$ mice, in the presence or absence of 4-OHT. These cells were then transplanted into syngeneic mice for accessing their leukemogenic potential. Complete *Cbx8* excision in the donor cells was achieved by 4-OHT treatment, as confirmed by genotyping the peripheral blood of the recipient mice 3 weeks post-transplant (Figure S3M). Consistent with our in vitro findings, mice receiving Cbx8-deficient, MLL-AF9-transduced cells failed to develop leukemia, whereas mice receiving WT MLL-AF9-transduced BM all died of leukemia, as evidenced by marked splenomegaly and extensive infiltration of peripheral blood, spleen, and liver (Figures 3H and 3J; Figure S3N). As expected, flow cytometry analysis showed that BM from the leukemic mice was replaced by GFP-positive, MLL-AF9-transformed cells (>99%). In contrast, BM from the mice receiving Cbx8-depleted donor cells was negative for GFP expression (Figure 3I). These results strongly demonstrate that CBX8 is required for MLL-AF9-induced leukemogenesis.

Notably, a previous study has shown that CBX8 also interacts with another MLL fusion partner, ENL, which is also a component of the EAP (or the related AEP) complex (Garcia-Cuellar et al., 2001). Therefore, it is likely that CBX8 is not only required for

MLL-AF9 leukemogenesis but also involved in leukemic transformation by other MLL fusion proteins that interact with the EAP (or the related AEP and the DotCom) complex, such as MLL-ENL. Indeed, similar to MLL-AF9, Cbx8 is essential for initiation and maintenance of leukemic transformation induced by MLL-ENL, as shown by BMT assays (Figures S3D–S3G). This finding suggests that the dependence on CBX8 of leukemic transformation is not restricted to MLL-AF9 but may apply to other MLL fusion proteins as well.

CBX8 Is Crucial for Proliferation and Survival of MLL-AF9-Transformed Leukemic Cells and for MLL-AF9-Induced Transcriptional Activation

To explore the underlying mechanisms of Cbx8-dependent oncogenic transformation, we first investigated whether the Cbx8 dependence is specific for certain MLL-rearranged transformation or for leukemic transformation in general. Using the conditional *Cbx8* knockout mice, we assessed the impact of Cbx8 deletion on leukemic transformation by E2A-HLF, a leukemogenic fusion protein that transforms through *Hox*-independent pathways (Ayton and Cleary, 2003). Despite the complete depletion of the Cbx8 protein achieved by 4-OHT treatment, neither the initiation nor the maintenance of E2A-HLF-induced leukemic transformation was affected, suggesting the specificity of Cbx8-dependent transformation (Figures S3H–S3L). Similar results were observed with Hoxa9/Meis1-transformed cells (data not shown). Together, these findings suggest that Cbx8 plays a specific role in leukemic transformation by certain MLL fusion proteins, such as MLL-AF9.

We then examined whether Cbx8 is important in regulating the proliferation of MLL-AF9 leukemic cells and found that the Cbx8 shRNA, but not the scrambled control, decreased the growth rate of MLL-AF9 leukemic cells (Figure 4A). The phenotype was even more dramatic in primary murine BM cells, where we observed a complete growth arrest in liquid-cultured, MLL-AF9-transformed BM cells (*Cbx8$^{f/f}$*; *Cre^{+}*) with *Cbx8* excision by 4-OHT treatment, whereas no such effect was observed in control cells (*Cbx8$^{f/f}$*; *Cre^{-}*) (Figures 4B and 4C). In agreement with these observations, the apoptotic population of MLL-AF9 leukemic cells increased upon Cbx8 depletion by 4-OHT treatment, but not in the control cells (Figure S4A). Additionally, we consistently observed a slight decrease of the S phase cell population upon Cbx8 depletion in MLL-AF9 leukemic cells (Figure S4B). However, the effect was rather minor, suggesting that the dramatic proliferation defect of MLL-AF9 cells upon Cbx8 depletion is not mainly due to cell-cycle arrest.

A well-established oncogenic mechanism of MLL-AF9 transformation is the constitutive activation of the *HOX* genes, particularly *HOXA9* along with the HOX cofactor *MEIS1* (Armstrong et al., 2002; Ayton and Cleary, 2003; Kumar et al., 2004), whereas CBX8 was previously shown to be involved in transcriptional repression (Dietrich et al., 2007; Maertens et al., 2009). The seemingly opposite effects of CBX8 and MLL-AF9 on transcriptional regulation raise an intriguing question: What role does CBX8 play in MLL-AF9-induced transcriptional activation? To address this question, we examined *Hoxa9* expression in MLL-AF9-transformed primary BM transduced with the Cbx8 shRNA. Compared to the control, Cbx8 downregulation led to a marked suppression of *Hoxa9* expression (Figure 4D). A similar effect was observed in MLL-AF9-transformed *Cbx8$^{f/f}$*; *Cre^{+}* BM, following *Cbx8* excision by 4-OHT treatment, but not in the control cells (Figure 4E; Figure S4C). To further confirm that the impact of Cbx8 on *Hoxa9* expression is dependent on the interaction between Cbx8 and MLL-AF9, we compared the *Hoxa9* expression in primary BM cells transduced by WT MLL-AF9 or by the mutants lacking the Cbx8 interaction (T542A and T554A). Notably, MLL-AF9 mutant-transduced cells show significantly reduced *Hoxa9* expression, compared to the cells transduced by WT MLL-AF9 (Figure 4F). It is noteworthy that the cells examined in this experiment were harvested after the second round of selection because very few mutant-transformed cells survived the third round of selection. Therefore, few residual nontransformed progenitors may account for the detected *Hoxa9* expression in the mutant-transformed cells, suggesting that the reduction of *Hoxa9* expression in the mutant-transduced cells could be even greater. Nevertheless, these data strongly indicate that Cbx8 serves as a coactivator of MLL-AF9, promoting *Hoxa9* upregulation in MLL-AF9-transformed cells. To further assess the specificity of the role of Cbx8 in *Hoxa9* transcriptional regulation, we examined the effect of Cbx8 knockdown on *Hoxa9* expression in several human and murine leukemic cell lines. CBX8-inducible knockdown stable cell lines were generated by lentiviral transduction of a TRIPZ-RFP-shCBX8 construct in three human leukemic cell lines. The THP-1 and Mono Mac 6 (MM6) cells are transformed by MLL-AF9, whereas K562 is a BCR-ABL-transformed cell line that serves as a control. As expected, knocking down of CBX8 induced by doxycycline treatment significantly decreased *HOXA9* expression in both MLL-AF9-transformed cell lines (MM6 and THP-1), but not in the control cell line (Figure S4D). Consistent with this observation, Cbx8 knockdown by shRNA led to a marked decrease of *Hoxa9* expression in a murine MLL-AF9 cell line, but not in the Hoxa9-independent E2A-HLF cell line (Figure S4E). These findings suggest that Cbx8 specifically contributes to MLL-AF9-induced *Hoxa9* transcriptional activation.

In order to mechanistically understand how Cbx8 facilitates MLL-AF9-induced *Hoxa9* upregulation, we investigated the effect of Cbx8 on *Hoxa9* promoter activity in the presence of MLL-AF9. We first performed dual luciferase assays in 293 cells transfected with a MLL-AF9 responsive luciferase construct, under the control of the murine *Hoxa9* promoter (*Hoxa9-LUC*). Our data show that disrupting the CBX8 interaction by the point mutation of T542A or T554A significantly decreased the activation of the *Hoxa9* promoter by MLL-AF9 (T542A: $p < 0.01$; T554A: $p < 0.01$; Figure 4G). Consistent with this result, knocking down the CBX8 level by siRNAs reduced the MLL-AF9-induced transcriptional activation by around 50% ($p < 0.01$; Figures 4H and 4I). Notably, neither the point mutations nor CBX8 knockdown significantly affected MLL-AF9 expression, indicating that the reduction in *Hoxa9* promoter activity was not due to a general decrease in the MLL-AF9 level (Figures S4F and S4G). A similar response was observed using another MLL-AF9 responsive luciferase reporter containing the *thymidine* kinase promoter and multimerized *Myc E* box, further supporting the importance of Cbx8 in MLL-AF9-induced transcriptional activation (Figures S4H and S4I). We then carried out chromatin immunoprecipitation (ChIP) in MLL-AF9-transformed murine

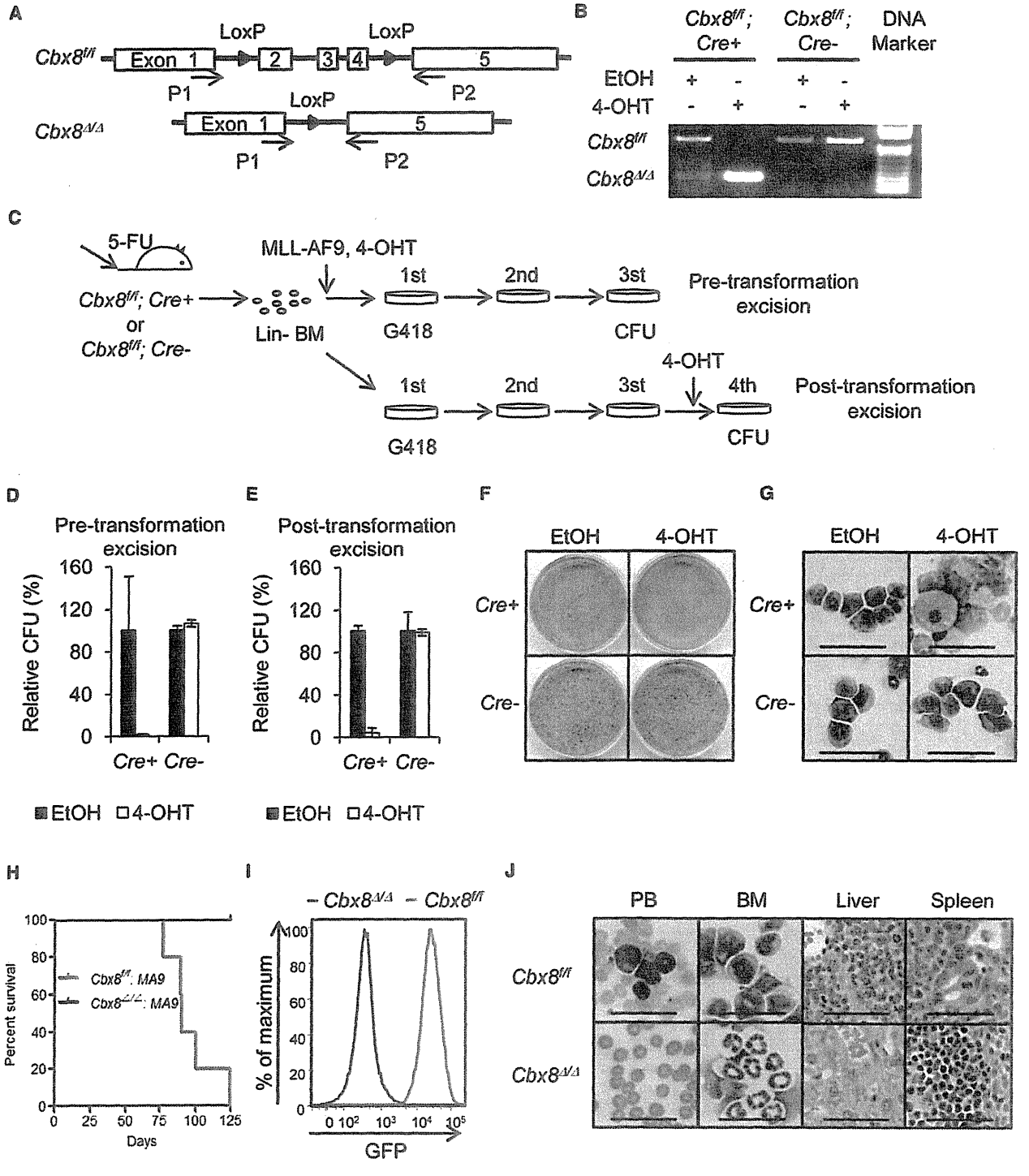

Figure 3. Cbx8 Is Required for Both Initiation and Maintenance of MLL-AF9 Leukemic Transformation

(A) Schematic showing the floxed *Cbx8* and the primers used for detecting the floxed and the excised *Cbx8*.

(B) Genotype analysis showing the efficiency of *Cbx8* excision induced by 4-OHT treatment in primary BM from *Cbx8*$^{f/f}$; *Cre*$^{+}$ mice, with ethanol treatment as a control (EtOH).

(C) Experimental scheme for the BMT assays with *Cbx8* excision in primary BM from *Cbx8*$^{f/f}$; *Cre*$^{+}$ and *Cbx8*$^{f/f}$; *Cre*$^{-}$ mice. The first experimental procedure was performed as described in Figure 2A, except that 4-OHT or ethanol was added during MLL-AF9 retroviral transduction. The second experiment was performed as described in Figure S2A, except using 4-OHT treatment instead of shCbx8 transduction.

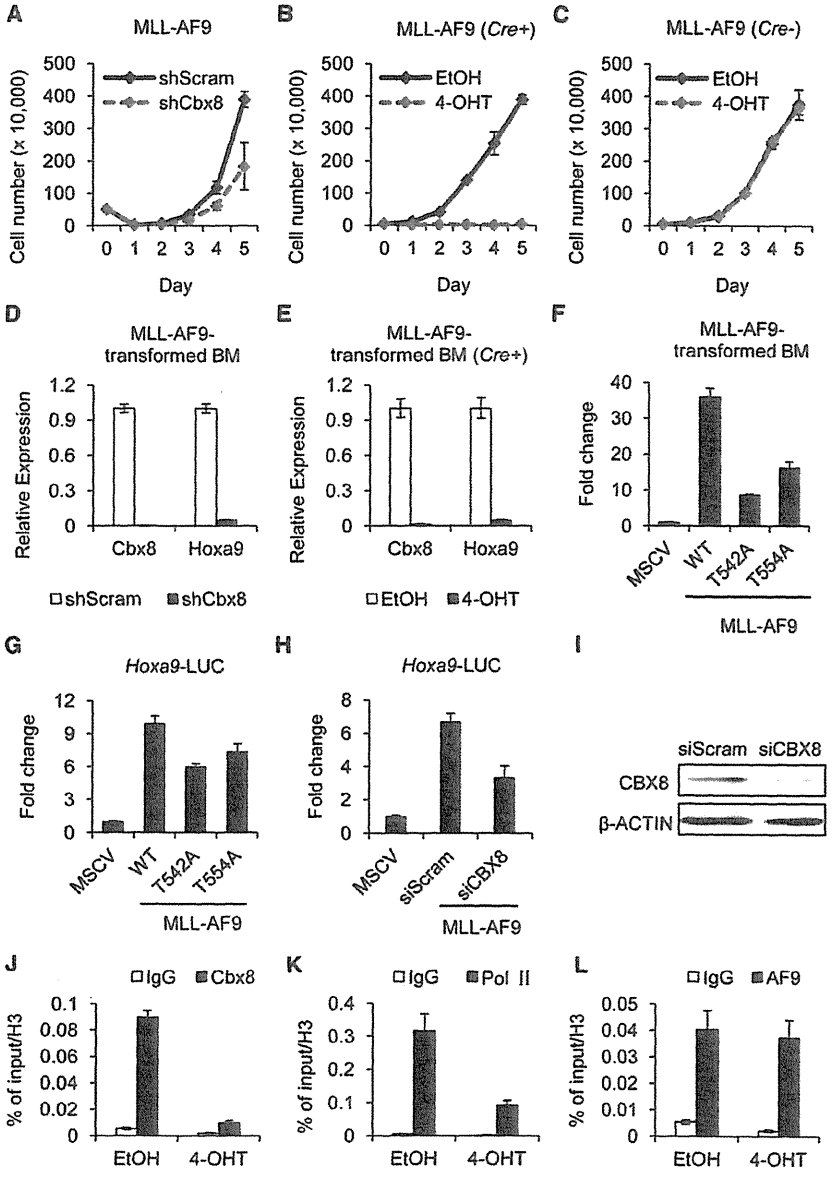

Figure 4. CBX8 Is Crucial for Proliferation and Survival of MLL-AF9-Transformed Leukemic Cells and for MLL-AF9-Induced Transcriptional Activation

(A) Growth curve of MLL-AF9 leukemic cells transduced with shCbx8 or control (shScram). Error bars represent ± SD from duplicate experiments. Results from one of three independent experiments are shown.

(B and C) Growth curves of MLL-AF9-transformed primary BM from *Cbx8*$^{f/f}$; *Cre*$^{+}$ and *Cbx8*$^{f/f}$; *Cre*$^{-}$ mice, with 4-OHT treatment compared to the control. Error bars represent ± SD from a duplicate experiment. Results from one of two independent experiments are shown.

(D) RT-PCR analysis of the expression of *Cbx8* and *Hoxa9* in MLL-AF9-transformed primary BM, with shCbx8 transduction compared to the control (shScram).

(E) RT-qPCR analysis of the expression of *Cbx8* and *Hoxa9* in MLL-AF9-transformed primary BM from *Cbx8*$^{f/f}$; *Cre*$^{+}$ mice, with 4-OHT treatment compared to the control (EtOH).

(F) RT-PCR analysis of the *Hoxa9* expression in primary BM transduced by WT MLL-AF9 or MLL-AF9 mutants, compared to the vector control. Error bars represent ±SD.

(G) Luciferase assay with a *Hoxa9* promoter-driven reporter activated by WT or mutant MLL-AF9 (T542A and T554A) in 293 cells. Error bars represent ± SD from three independent experiments.

(H) Luciferase assay with the *Hoxa9* promoter-driven reporter activated by MLL-AF9, with CBX8 knockdown (siCBX8) or control treatment (siScram) in HeLa cells. Error bars represent ± SD from three independent experiments.

(I) Western blot showing CBX8 expression with siCBX8 treatment compared to the control (siScram).

(J–L) Relative binding of Cbx8, RNAP II, and MLL-AF9 together with WT AF9 to the *Hoxa9* promoter in MLL-AF9-transformed cells from *Cbx8*$^{f/f}$; *Cre*$^{+}$ mice, with 4-OHT treatment compared to the control (EtOH).

See also Figure S4.

hematopoietic cells to examine changes at the *Hoxa9* promoter in response to Cbx8 depletion. In agreement with the suppression of *Hoxa9* activation, a significant decrease of RNA polymerase II (RNAP II) binding to the *Hoxa9* promoter was detected following Cbx8 depletion by 4-OHT treatment, whereas as expected, Cbx8 binding was essentially ablated (Figures 4J and 4K). Moreover, the collective binding of MLL-AF9 fusion protein and WT AF9 was not affected by Cbx8 depletion, as shown by ChIP using an anti-AF9 antibody (Figure 4L). Because WT AF9 is also a component of the MLL-AF9 complex, and our previous results already showed that the Cbx8 interaction is not required for the assembly between the EAP complex and the MLL-AF9 fusion protein (Figures 1F and 1G; Figures S1C and S1D), this observation suggests that the recruitment of the MLL-AF9

(D and E) Relative CFU of MLL-AF9-transduced cells in the two experimental settings. Error bars represent ± SD from two independent experiments.

(F) Representative INT-stained colonies in methylcellulose.

(G) Wright-Giemsa-stained cells isolated after transformation selection. Scale bars, 50 μm.

(H) Kaplan-Meier survival analysis of mice transplanted with *Cbx8*$^{4/4}$ (n = 5) or *Cbx8*$^{f/f}$ (n = 5) donor BM.

(I) GFP expression of BM from the transplanted mice, assessed by flow cytometry.

(J) Wright-Giemsa staining of peripheral blood (PB) smear and BM and histology of liver and spleen from the transplanted mice. Scale bar, 50 μm.

See also Figure S3.

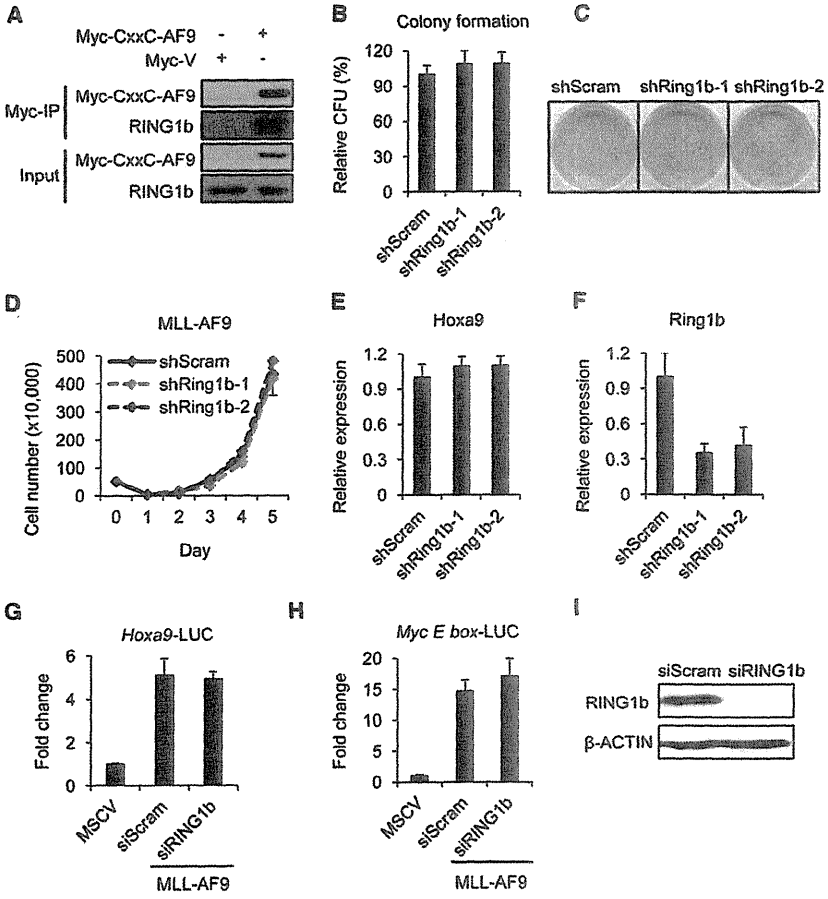

Figure 5. Ring1b Knockdown Does Not Recapitulate the Effects of Cbx8 Knockdown in MLL-AF9 Leukemic Transformation

(A) coIP of endogenous RING1b with Myc-CxxC-AF9 in 293 cells. A fraction (3%) of cell lysate was used for input control.

(B) Relative CFU of MLL-AF9 leukemic cells with Ring1b knockdown by two individual shRing1b molecules, compared to the control (shScram). Error bars represent ± SD from three independent experiments.

(C) Representative INT-stained colonies in methylcellulose.

(D) Growth curve of MLL-AF9 leukemic cells with Ring1b knockdown, compared to the control. Error bars represent ± SD from a duplicate experiment. Results from one of three independent experiments are shown.

(E) RT-PCR analysis of *Hoxa9* expression in MLL-AF9 leukemic cells with Ring1b knockdown, compared to the control.

(F) RT-PCR analysis of *Ring1b* expression in MLL-AF9 leukemic cells, confirming the knockdown efficiency. Error bars represent ±SD.

(G and H) Experiments were performed as described in Figures 4H and S4I, except using siRNAs specifically targeting RING1b (siRING1b) in place of siCBX8. Error bars represent ± SD from three independent experiments.

(I) Western blot showing RING1b expression with siRING1b treatment, compared to the control (siScram).

See also Figure S5.

complex to the *Hoxa9* promoter is not significantly affected by the loss of Cbx8, which is also consistent with previous reports regarding the importance of the retained MLL portion in MLL fusion complex localization, rather than the fusion partner portion (Ayton et al., 2004; Milne et al., 2010; Muntean et al., 2010; Slany et al., 1998; Yokoyama and Cleary, 2008). Similar findings were observed using CBX8-inducible knockdown MLL-AF9-transformed cell lines (Figures S4J–S4M), further supporting that Cbx8 regulates MLL-AF9 target promoter activity, thereby contributing to MLL-AF9-induced transcriptional activation, without affecting the collective localization of MLL-AF9 and WT AF9.

Role of CBX8 in MLL-AF9 Leukemic Transformation and Transcriptional Activation Is Independent of PRC1

To date, the only reported functional characterization of Cbx8 is its role as a transcriptional repressor in PRC1, whereas our data indicate that Cbx8 serves as a transcriptional coactivator in the presence of MLL-AF9. These opposing transcriptional regulatory roles suggest that Cbx8 functions in a PRC1-independent manner in MLL-AF9 leukemic transformation. It has been shown that Ring1b, another PRC1 component, is required for the stability of PRC1 complexes (Leeb and Wutz, 2007; van der Stoop et al., 2008). In addition, previous studies have indicated that Ring1b also interacts with AF9 (Monroe et al., 2011), which we confirmed by IP experiments showing that endogenous RING1b consistently coprecipitates with the MLL-AF9 fragment, CxxC-AF9 (Figure 5A). Therefore, to test our hypothesis of the potential PRC1-independent function of Cbx8, we first assessed the impact of Ring1b on MLL-AF9 leukemic transformation by BMT assays. Two individual shRNA molecules specifically targeting *Ring1b* were used to effectively knock down *Ring1b* expression in MLL-AF9-transformed leukemic cells. Reduction in *Ring1b* expression in these experiments did not impair the transformation ability of MLL-AF9 (Figures 5B, 5C, and 5F). Knocking down *Ring1b* did not significantly affect the growth rate or *Hoxa9* expression in MLL-AF9 cells either (Figures 5D and 5E). We also performed dual luciferase assays to examine the impact of knocking down RING1b by siRNA on the MLL-AF9 target promoter activity. Despite the marked reduction of RING1b expression shown by western blot analysis, MLL-AF9-induced transactivation of the target promoters was not suppressed by RING1b knockdown (Figures 5G–5I). Similar to our observations with Ring1b, knockdown of Bmi1, another core PRC1 component, did not affect the transformation ability, growth rate, or transcriptional activation in MLL-AF9 leukemic cells (Figures S5B–S5I). Consistent with these observations, Cbx8 depletion in MLL-AF9-transformed BM cells did not affect the global levels of Ring1b and Bmi1, as shown by western blot analysis (Figure S5A). Taken together, these findings suggest

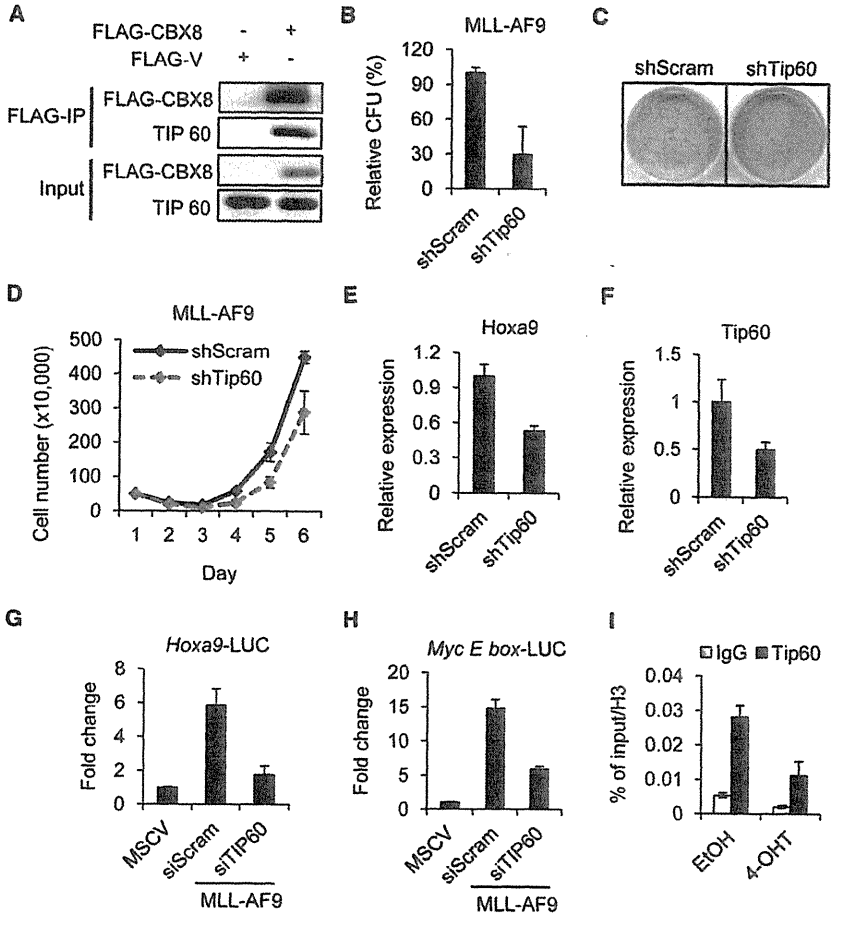

Figure 6. CBX8 Regulates the Localization of TIP60, Whose Downregulation Phenocopies the Effects of Cbx8 Knockdown in MLL-AF9 Leukemic Transformation

(A) coIP of endogenous TIP60 with FLAG-CBX8 in 293 cells, after Benzonase treatment. A fraction (3%) of cell lysate was used for input control.

(B) Relative CFU of MLL-AF9 leukemic cells with Tip60 knockdown by shRNA, compared to the control (shScram). Error bars represent ± SD from three independent experiments.

(C) Representative INT-stained colonies in methylcellulose.

(D) Growth curve of MLL-AF9 leukemic cells with Tip60 knockdown, compared to the control. Error bars represent ± SD from a duplicate experiment. Results from one of three independent experiments are shown.

(E) RT-PCR analysis of *Hoxa9* expression in MLL-AF9 leukemic cells with Tip60 knockdown, compared to the control.

(F) RT-PCR analysis of *Tip60* expression in MLL-AF9 leukemic cells, showing the knockdown efficiency. Error bars represent ±SD.

(G and H) Experiments were performed as described in Figures 4H and S4I, except using siRNAs specifically targeting TIP60 (siTIP60) instead of siCBX8. Error bars represent ± SD from three independent experiments.

(I) Relative binding of Tip60 to the *Hoxa9* promoter in MLL-AF9-transformed cells from *Cbx8*$^{fl/fl}$; *Cre*$^{+}$ mice, with *Cbx8* excision induced by 4-OHT treatment compared to the control (EtOH). Error bars represent ±SD.

See also Figure S6.

that Cbx8 functions as an MLL-AF9 cofactor to promote leukemogenesis in a PRC1-independent manner.

Notably, given the finding that CBX8 is involved in the *INK4a/ARF* transcriptional repression by PRC1 in fibroblasts (Dietrich et al., 2007), it is important to determine whether the observed effect of CBX8 on MLL-AF9 transcriptional activation is related to its role in *INK4a/ARF* regulation. Therefore, we examined the impact of Cbx8 on *Ink4a/Arf* expression by RT-PCR in MLL-AF9 leukemic cells. Neither downregulation nor depletion of Cbx8 led to *Ink4a/Arf* activation (Figures S8A and S8B), confirming that the Cbx8-dependent MLL-AF9 transformation is not due to *Ink4a/Arf* repression.

CBX8 Regulation of TIP60 Localization Contributes to MLL-AF9 Leukemic Transformation

The characterization of the PRC1 independence of Cbx8 functions in MLL-AF9 leukemic transformation prompted us to explore the possible involvement of other Cbx8-interacting proteins that may explain the role of Cbx8 in transcriptional activation. A previous study has reported that CBX8 directly interacts with the histone acetyltransferase HIV *T*at-*i*nteracting *p*rotein of *60* kDa (TIP60) by high-throughput yeast two-hybrid screens and mass spectroscopy analysis (Stelzl et al., 2005). However, this observation has not yet been verified in any mammalian cell system; therefore, the functional implication of this interaction remains an open question. To first confirm this interaction, we transiently expressed FLAG-tagged CBX8 in 293 cells. Specific interaction between CBX8 and TIP60 was detected by IP experiments: using an anti-FLAG antibody to pull down CBX8, we observed that CBX8 consistently coprecipitated with endogenous TIP60 in the presence of Benzonase, indicating that CBX8 interacts with TIP60 in a DNA-independent manner (Figure 6A; Figure S6A). This finding implied an intriguing possibility that CBX8 promotes MLL-AF9 leukemic transformation, at least partially through its interaction with the transcriptional coactivator TIP60. To test this hypothesis, we first assessed the impact of Tip60 on MLL-AF9 leukemic transformation by BMT assays. Using shRNA molecules specifically targeting Tip60, we observed a reduction in the colony formation ability of MLL-AF9 leukemic cells (Figures 6B, 6C, and 6F). Moreover, Tip60 downregulation by shRNA led to a decrease in the growth rate and *Hoxa9* expression of MLL-AF9-transformed cells (Figures 6D and 6E). Similar results were obtained using a different shRNA pool, further supporting that Tip60 positively contributes to MLL-AF9 leukemic transformation (Figures S6B–S6F).

To further characterize the role of Tip60 in MLL-AF9-induced transcriptional activation, we performed dual luciferase assays to examine the impact of TIP60 downregulation by siRNA on the MLL-AF9 target promoter activity. A significant reduction of TIP60 expression was confirmed by western blot analysis

(Figure S6G). As expected, the MLL-AF9-induced transcriptional activation of the target promoters was significantly suppressed by TIP60 knockdown (Figures 6G and 6H). Collectively, these data demonstrate that knocking down Tip60 phenocopies the effect of Cbx8 knockdown in MLL-AF9 leukemic cells, suggesting a functional significance of the CBX8/TIP60 interaction in MLL-AF9 leukemic transformation. To confirm that the observed role of Tip60 is indeed associated with the Cbx8/Tip60 interaction, we performed ChIP assays in MLL-AF9-transformed leukemic cells, following Cbx8 depletion by 4-OHT treatment. As expected, Cbx8 depletion resulted in decreased Tip60 binding at the *Hoxa9* promoter (Figure 6I). Similar findings were seen using MLL-AF9-transformed cell lines, MM6 and THP-1, engineered for inducible knockdown of CBX8. In these cells, TIP60 binding at the *HOXA9* promoter was reduced upon CBX8 downregulation induced by doxycycline treatment (Figure S6; data not shown). Together, our results suggest that CBX8 regulates the localization of TIP60, which plays a positive role in MLL-AF9 leukemic transformation. Of note, Tip60 downregulation in MLL-AF9 leukemic cells did not lead to *Ink4a/Arf* activation (Figures S8C and S8D), consistent with previous observations from Cbx8 knockdown, further supporting that *Ink4a/Arf* repression does not account for the role of Cbx8 in MLL-AF9 leukemogenesis.

Cbx8 Is Not Required for Normal Hematopoiesis

The profound impact of Cbx8 on MLL-AF9 leukemogenesis prompted us to examine the role of Cbx8 in normal hematopoiesis. We first examined the effect of Cbx8 depletion on hematopoietic steady-state conditions in vivo. Constitutive depletion of Cbx8 showed no aberrant phenotype, and deletion of Cbx8 by 4-OHT treatment in adult animals had no detectable effect on any measured peripheral blood population as assessed by complete blood count (CBC) analysis (Figures 7A–7D; Figure S7A). Moreover, both the cellularity of major hematopoietic organs (BM, spleen, and thymus) and the cell numbers of mature hematopoietic populations as defined by flow cytometry were similar between Cbx8-deficient mice and controls (Figures 7E–7H; Figures S7C–S7E). To address potential effects of Cbx8 deletion on primitive long-term hematopoietic stem cells (LT-HSCs), we combined flow cytometry for characterization of progenitor populations and competitive BM transplantation assays. These analyses revealed no detectable differences in LT-HSC numbers (Figure 7I) or hematopoietic reconstitution ability of Cbx8 WT or deficient BM in lethally irradiated recipients (Figure 7K). In addition, the total progenitor output from the BM of Cbx8-deficient animals was similar to controls, as measured by colony-forming assays (Figure 7J; Figure S7B). Together, these findings indicate that Cbx8 is not required for steady-state hematopoiesis, LT-HSC maintenance, or stem and progenitor cell function.

DISCUSSION

Our study establishes CBX8 as an essential cofactor required for MLL-AF9-induced transcriptional activation and leukemic transformation (Figure 8). CBX8 is one of the five human homologs of the *Drosophila* Pc protein. Although all CBX proteins share highly conserved chromodomains and Pc boxes, their different sizes and the presence of other motifs suggest potentially different functions (Whitcomb et al., 2007). Indeed, previous studies have reported that mice deficient for different PRC1 components show only a partial overlap in phenotype, raising the possibility of PRC1-independent functions of these components that may be context dependent and involve other protein complexes (de Napoles et al., 2004; Katoh-Fukui et al., 1998; Leeb and Wutz, 2007; Suzuki et al., 2002; Voncken et al., 2003). The present study has uncovered such a PRC1-independent function of CBX8 in MLL-AF9-induced transcriptional regulation. Interestingly, contrary to its role as a transcriptional repressor in PRC1, CBX8 serves as a transcriptional coactivator in the MLL-AF9 complex. Furthermore, CBX8 is present in the EAP (or the related AEP and the DotCom) transcriptional activation complex (Mohan et al., 2010a; Monroe et al., 2011; Yokoyama et al., 2010) and is also required for the leukemic transformation induced by MLL-ENL, another EAP-interacting MLL fusion protein, implying a broader role of CBX8 in MLL-rearranged leukemogenesis, which warrants further exploration. Importantly, consistent with our observations, a recent study showed that Bmi1 is not required for MLL-AF9-induced leukemogenesis (Smith et al., 2011). Moreover, our findings that neither Cbx8 downregulation or depletion nor Tip60 knockdown induced *Ink4a/Arf* expression further support that the role of CBX8 in MLL-AF9 leukemogenesis is independent of PRC1.

In addition to the MLL fusion partners, CBX8 has previously been shown to directly interact with the HAT TIP60 (Stelzl et al., 2005). Tip60 is a member of the MYST (*M*oz, *Y*bf2/Sas3, *S*as2, *T*ip60) protein family, the largest family of HATs that is present in all eukaryotes (Voss and Thomas, 2009). Histone acetylation near promoters is associated with transcriptional activation; therefore, HATs generally promote transcriptional activation (Mills, 2010). Several TrxG complexes are known to recruit HATs during normal development. For example, the HAT MYST1 has been purified in WT MLL complex, and the HAT CREB-binding protein (CBP) is known to interact with both MLL and another TrxG protein ASH1 (Bantignies et al., 2000; Dou et al., 2005; Ernst et al., 2001; Petruk et al., 2001). Under normal physiological conditions, HATs function as a coactivator to facilitate TrxG-induced transcriptional activation, antagonizing the transcriptional repressive effect of the PcG complex (Mills, 2010; Pasini et al., 2010). This mechanism contributes to the active *HOXA9* expression in hematopoietic stem cells and early progenitors (Figure 8). Moreover, MLL is fused to CBP or P300 in a subset of acute leukemias (Wang et al., 2005). However, previous studies have not reported HATs as a component of the EAP complex, which is recruited by the most common MLL fusion partners. Therefore, whether HATs contribute to transcriptional activation induced by common MLL-rearranged oncoproteins remains unknown. Our finding of the CBX8-dependent TIP60 localization at the *HOXA9* promoter indicates that this transcriptional activation mechanism is likely to be adopted by MLL fusion proteins to activate target gene expression, such as *HOXA9*. Interestingly, a previous RNAi screening study in mouse embryonic stem cells (ESCs) showed that Tip60 is required for pluripotency, whereas MLL myeloid leukemia stem cells have been shown to share the transcriptional program with ESCs, rather than adult stem cells (Fazzio et al., 2008; Somervaille et al., 2009). Together,

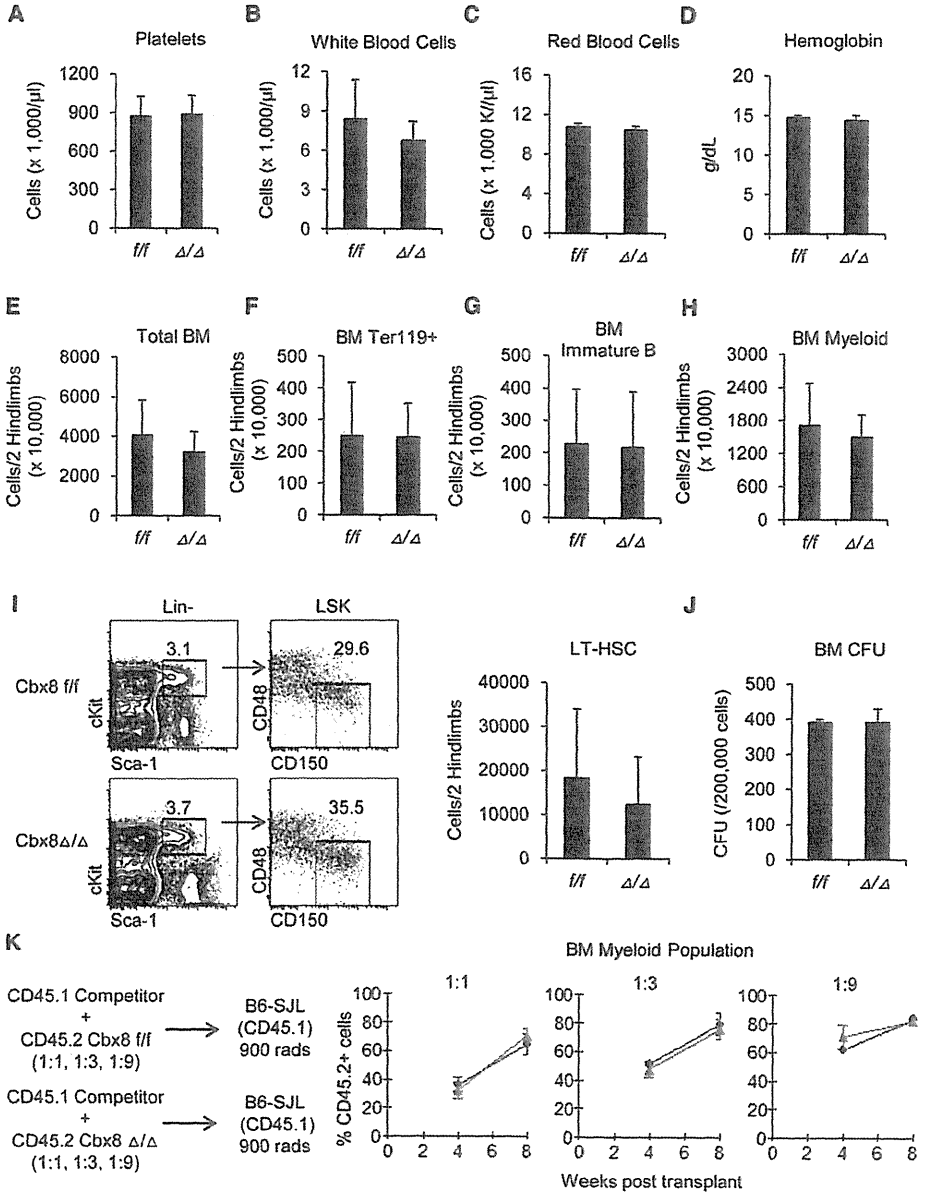

Figure 7. Cbx8-Depleted Mice Show Normal Hematopoiesis

(A–D) Peripheral blood CBC analysis of (A) platelets, (B) white blood cells, (C) red blood cells, and (D) hemoglobin content of *Cbx8* floxed (*f/f*) and deleted (*Δ/Δ*) mice. The experiment was performed 4 weeks after complete *Cbx8* excision in vivo.

(E–H) Absolute quantification of total BM cellularity (E), erythroid cells (Ter119+; F), developing B lymphocytes (AA4.1+CD19+B220+; G), and myeloid cells (CD11b+Gr1+; H) from $Cbx8^{f/f}$ and $Cbx8^{\Delta/\Delta}$, analyzed by flow cytometry (error bars represent mean + SD; n = 5 mice/genotype).

(I) Flow cytometric analysis of LT-HSCs (CD150+CD48-LSK) from $Cbx8^{f/f}$ and $Cbx8^{\Delta/\Delta}$ mice (error bars represent mean + SD; n = 5 mice/genotype).

(J) Colony-forming assays using BM from $Cbx8^{f/f}$ and $Cbx8^{\Delta/\Delta}$ mice. The data included four independent experiments per genotype (error bars represent mean + SD; n = 3 plate/experiment).

(K) Competitive BM transplantation at competitor: tester ratios of 1:1 (n = 10/group), 1:3 (n = 5 mice per group), and 1:9 (n = 5 mice per group). No difference between $Cbx8^{f/f}$ and $Cbx8^{\Delta/\Delta}$ mice was observed in tester contribution to myeloid reconstitution at any ratio (data represent mean ± SD).

(E)–(K) were performed 5–7 months after complete *Cbx8* excision in vivo.

See also Figure S7.

these observations suggest a possible functional association between the TIP60-regulated signaling network and the transcriptional program in MLL-rearranged leukemic cells, raising the possibility that TIP60 may be involved in establishing the transcriptional program required for MLL-AF9-induced leukemogenesis (Figure 8). Given the broad involvement of TIP60 in

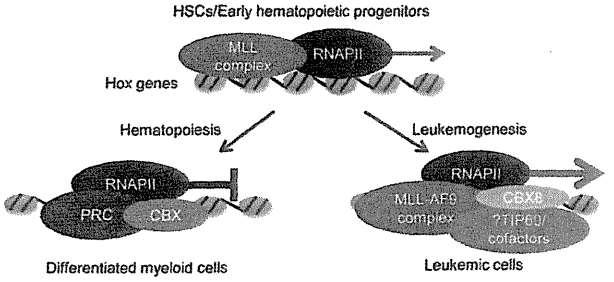

Figure 8. Schematic Model Illustrating Role of CBX8 in Promoting MLL-AF9-Induced Leukemogenesis

Top view shows that recruitment of WT MLL is required for transcriptional regulation of *Hox* gene expression in HSCs and early progenitor cells. Left view illustrates that during normal hematopoiesis, *Hox* gene expression decreases due to the transcriptional repression of PcG proteins. Right view shows that In MLL-AF9 leukemic cells, CBX8 interacts with MLL-AF9 at the target gene loci to facilitate transcriptional activation, possibly by recruiting transcriptional cofactors such as TIP60, thereby promoting leukemogenesis. See also Figure S8.

multiple biological processes (Sapountzi et al., 2006), it is unclear whether the role of TIP60 in MLL-AF9 leukemogenesis is as specific as that of CBX8. This mechanism warrants further investigation. Finally, our identification of the critical role of the CBX8/MLL-AF9 interaction in leukemogenesis but not viability or normal hematopoiesis suggests that developing small molecule inhibitors targeting CBX8 represents a promising therapeutic strategy for MLL-rearranged leukemias.

EXPERIMENTAL PROCEDURES

Cell Culture and Animal Use

HeLa and 293 cells were cultured in Dulbecco's modified Eagle's medium (DMEM) supplemented with 10% fetal bovine serum (FBS) and nonessential amino acids. MLL-AF9, MLL-ENL, and E2A-HLF cells were cultured in Iscove's modified Dulbecco's medium (IMDM) supplemented with 15% fetal calf serum (FCS; STEMCELL Technologies). THP-1, MM6, and K562 cells were cultured in RPMI-1640 medium supplemented with 10% FBS. The Tripz-RFP-shCBX8 expression was induced by 0.5 μg/ml doxycycline. Full details of conditional gene targeting of *Cbx8* and analysis of $Cbx8^{-/-}$ embryos will be provided in a subsequent manuscript (H.K., unpublished data). All animal experiments in this study were approved by the University of Michigan Committee on Use and Care of Animals and Unit for Laboratory Animal Medicine (ULAM).

In Vivo Leukemogenesis Assays

Lin- BM was isolated from 6- to 8-week-old mice ($Cbx8^{f/f}$; Cre^{+}) injected with 5-fluorouacil (see Supplemental Experimental Procedures). The harvested Lin- BM cells were retrovirally transduced with MigR1-MLL-AF9 by two rounds of spinoculation in the presence of either 4-OHT (100 nM) or ethanol as a control. The cells were then counted and injected intravenously through the tail vein to cohorts of lethally irradiated (900 rads) C57BL/6 mice (3.5×10^4 cells per injection). Recipient mice were maintained on antibiotics for 2 weeks after transplantation.

CBC Analysis

For in vivo *Cbx8* excision, $Cbx8^{f/f}$; Cre^{+} mice were treated with corn oil or 50 mg/kg 4-OHT by i.p. injection for 5 continuous days. Four weeks after injection, peripheral blood was used harvested in EDTA (ethylenediaminetetraacetic acid)-containing Microtainer tubes (BD Biosciences) and subjected for analysis performed by the ULAM laboratory. Meanwhile, genotyping was performed using genomic DNA extracted from peripheral blood.

Flow Cytometry and Cell Sorting

After blocking nonspecific binding with unlabeled rat plus mouse IgG (Sigma-Aldrich), cells were stained on ice in PBS plus 4% FCS and sorted on FACSAria (BD Biosciences). Analysis was performed on LSR II, FACSCanto, or FACSAria (BD Biosciences). Files were analyzed in FlowJo (TreeStar).

Statistical Analysis

Statistical significance was determined by Student's t test using the Excel software (Microsoft 2007); $p < 0.05$ was considered statistically significant.

SUPPLEMENTAL INFORMATION

Supplemental Information includes eight figures and Supplemental Experimental Procedures and can be found with this article online at doi:10.1016/j.ccr.2011.09.008.

ACKNOWLEDGMENTS

We thank Ann Friedman and Julien Schira for technical assistance. J.L.H. is supported by the National Institutes of Health (R01-CA92251) and by a SCOR grant from the Leukemia and Lymphoma Society (Jonathan Licht: PI).

Received: November 25, 2010
Revised: July 21, 2011
Accepted: September 20, 2011
Published: November 14, 2011

REFERENCES

Aplan, P.D. (2006). Chromosomal translocations involving the MLL gene: molecular mechanisms. DNA Repair (Amst.) *5*, 1265–1272.

Armstrong, S.A., Staunton, J.E., Silverman, L.B., Pieters, R., den Boer, M.L., Minden, M.D., Sallan, S.E., Lander, E.S., Golub, T.R., and Korsmeyer, S.J. (2002). MLL translocations specify a distinct gene expression profile that distinguishes a unique leukemia. Nat. Genet. *30*, 41–47.

Ayton, P.M., and Cleary, M.L. (2003). Transformation of myeloid progenitors by MLL oncoproteins is dependent on Hoxa7 and Hoxa9. Genes Dev. *17*, 2298–2307.

Ayton, P.M., Chen, E.H., and Cleary, M.L. (2004). Binding to nonmethylated CpG DNA is essential for target recognition, transactivation, and myeloid transformation by an MLL oncoprotein. Mol. Cell. Biol. *24*, 10470–10478.

Bantignies, F., Goodman, R.H., and Smolik, S.M. (2000). Functional interaction between the coactivator *Drosophila* CREB-binding protein and ASH1, a member of the trithorax group of chromatin modifiers. Mol. Cell. Biol. *20*, 9317–9330.

Bárdos, J.I., Saurin, A.J., Tissot, C., Duprez, E., and Freemont, P.S. (2000). HPC3 is a new human polycomb orthologue that interacts and associates with RING1 and Bmi1 and has transcriptional repression properties. J. Biol. Chem. *275*, 28785–28792.

Cheung, N., Chan, L.C., Thompson, A., Cleary, M.L., and So, C.W. (2007). Protein arginine-methyltransferase-dependent oncogenesis. Nat. Cell Biol. *9*, 1208–1215.

de Napoles, M., Mermoud, J.E., Wakao, R., Tang, Y.A., Endoh, M., Appanah, R., Nesterova, T.B., Silva, J., Otte, A.P., Vidal, M., et al. (2004). Polycomb group proteins Ring1A/B link ubiquitylation of histone H2A to heritable gene silencing and X inactivation. Dev. Cell *7*, 663–676.

Dietrich, N., Bracken, A.P., Trinh, E., Schjerling, C.K., Koseki, H., Rappsilber, J., Helin, K., and Hansen, K.H. (2007). Bypass of senescence by the polycomb group protein CBX8 through direct binding to the INK4A-ARF locus. EMBO J. *26*, 1637–1648.

Dou, Y., and Hess, J.L. (2008). Mechanisms of transcriptional regulation by MLL and its disruption in acute leukemia. Int. J. Hematol. *87*, 10–18.

Dou, Y., Milne, T.A., Tackett, A.J., Smith, E.R., Fukuda, A., Wysocka, J., Allis, C.D., Chait, B.T., Hess, J.L., and Roeder, R.G. (2005). Physical association and coordinate function of the H3 K4 methyltransferase MLL1 and the H4 K16 acetyltransferase MOF. Cell *121*, 873–885.

Ernst, P., Wang, J., Huang, M., Goodman, R.H., and Korsmeyer, S.J. (2001). MLL and CREB bind cooperatively to the nuclear coactivator CREB-binding protein. Mol. Cell. Biol. *21*, 2249–2258.

Fazzio, T.G., Huff, J.T., and Panning, B. (2008). An RNAi screen of chromatin proteins identifies Tip60-p400 as a regulator of embryonic stem cell identity. Cell *134*, 162–174.

García-Cuéllar, M.P., Zilles, O., Schreiner, S.A., Birke, M., Winkler, T.H., and Slany, R.K. (2001). The ENL moiety of the childhood leukemia-associated MLL-ENL oncoprotein recruits human Polycomb 3. Oncogene *20*, 411–419.

Hemenway, C.S., de Erkenez, A.C., and Gould, G.C. (2001). The polycomb protein MPc3 interacts with AF9, an MLL fusion partner in t(9;11)(p22;q23) acute leukemias. Oncogene *20*, 3798–3805.

Katoh-Fukui, Y., Tsuchiya, R., Shiroishi, T., Nakahara, Y., Hashimoto, N., Noguchi, K., and Higashinakagawa, T. (1998). Male-to-female sex reversal in M33 mutant mice. Nature *393*, 688–692.

Kerppola, T.K. (2009). Polycomb group complexes—many combinations, many functions. Trends Cell Biol. *19*, 692–704.

Krivtsov, A.V., and Armstrong, S.A. (2007). MLL translocations, histone modifications and leukaemia stem-cell development. Nat. Rev. Cancer *7*, 823–833.

Krivtsov, A.V., Feng, Z., Lemieux, M.E., Faber, J., Vempati, S., Sinha, A.U., Xia, X., Jesneck, J., Bracken, A.P., Silverman, L.B., et al. (2008). H3K79 methylation profiles define murine and human MLL-AF4 leukemias. Cancer Cell *14*, 355–368.

Kumar, A.R., Hudson, W.A., Chen, W., Nishiuchi, R., Yao, Q., and Kersey, J.H. (2004). Hoxa9 influences the phenotype but not the incidence of Mll-AF9 fusion gene leukemia. Blood *103*, 1823–1828.

Lavau, C., Szilvassy, S.J., Slany, R., and Cleary, M.L. (1997). Immortalization and leukemic transformation of a myelomonocytic precursor by retrovirally transduced HRX-ENL. EMBO J. *16*, 4226–4237.

Leeb, M., and Wutz, A. (2007). Ring1B is crucial for the regulation of developmental control genes and PRC1 proteins but not X inactivation in embryonic cells. J. Cell Biol. *178*, 219–229.

Lin, C., Smith, E.R., Takahashi, H., Lai, K.C., Martin-Brown, S., Florens, L., Washburn, M.P., Conaway, J.W., Conaway, R.C., and Shilatifard, A. (2010). AFF4, a component of the ELL/P-TEFb elongation complex and a shared subunit of MLL chimeras, can link transcription elongation to leukemia. Mol. Cell *37*, 429–437.

Maertens, G.N., El Messaoudi-Aubert, S., Racek, T., Stock, J.K., Nicholls, J., Rodriguez-Niedenführ, M., Gil, J., and Peters, G. (2009). Several distinct polycomb complexes regulate and co-localize on the INK4a tumor suppressor locus. PLoS One *4*, e6380.

Mills, A.A. (2010). Throwing the cancer switch: reciprocal roles of polycomb and trithorax proteins. Nat. Rev. Cancer *10*, 669–682.

Milne, T.A., Kim, J., Wang, G.G., Stadler, S.C., Basrur, V., Whitcomb, S.J., Wang, Z., Ruthenburg, A.J., Elenitoba-Johnson, K.S., Roeder, R.G., and Allis, C.D. (2010). Multiple interactions recruit MLL1 and MLL1 fusion proteins to the HOXA9 locus in leukemogenesis. Mol. Cell *38*, 853–863.

Mohan, M., Lin, C., Guest, E., and Shilatifard, A. (2010a). Licensed to elongate: a molecular mechanism for MLL-based leukaemogenesis. Nat. Rev. Cancer *10*, 721–728.

Mohan, M., Herz, H.M., Takahashi, Y.H., Lin, C., Lai, K.C., Zhang, Y., Washburn, M.P., Florens, L., and Shilatifard, A. (2010b). Linking H3K79 trimethylation to Wnt signaling through a novel Dot1-containing complex (DotCom). Genes Dev. *24*, 574–589.

Monroe, S.C., Jo, S.Y., Sanders, D.S., Basrur, V., Elenitoba-Johnson, K.S., Slany, R.K., and Hess, J.L. (2011). MLL-AF9 and MLL-ENL alter the dynamic association of transcriptional regulators with genes critical for leukemia. Exp Hematol. *39*, 77–86.

Mueller, D., Bach, C., Zeisig, D., Garcia-Cuellar, M.P., Monroe, S., Sreekumar, A., Zhou, R., Nesvizhskii, A., Chinnaiyan, A., Hess, J.L., and Slany, R.K. (2007). A role for the MLL fusion partner ENL in transcriptional elongation and chromatin modification. Blood *110*, 4445–4454.

Muntean, A.G., Tan, J., Sitwala, K., Huang, Y., Bronstein, J., Connelly, J.A., Basrur, V., Elenitoba-Johnson, K.S., and Hess, J.L. (2010). The PAF complex synergizes with MLL fusion proteins at HOX loci to promote leukemogenesis. Cancer Cell *17*, 609–621.

Nakamura, T., Mori, T., Tada, S., Krajewski, W., Rozovskaia, T., Wassell, R., Dubois, G., Mazo, A., Croce, C.M., and Canaani, E. (2002). ALL-1 is a histone methyltransferase that assembles a supercomplex of proteins involved in transcriptional regulation. Mol. Cell *10*, 1119–1128.

Pasini, D., Malatesta, M., Jung, H.R., Walfridsson, J., Willer, A., Olsson, L., Skotte, J., Wutz, A., Porse, B., Jensen, O.N., and Helin, K. (2010). Characterization of an antagonistic switch between histone H3 lysine 27 methylation and acetylation in the transcriptional regulation of Polycomb group target genes. Nucleic Acids Res. *38*, 4958–4969.

Petruk, S., Sedkov, Y., Smith, S., Tillib, S., Kraevski, V., Nakamura, T., Canaani, E., Croce, C.M., and Mazo, A. (2001). Trithorax and dCBP acting in a complex to maintain expression of a homeotic gene. Science *294*, 1331–1334.

Sapountzi, V., Logan, I.R., and Robson, C.N. (2006). Cellular functions of TIP60. Int. J. Biochem. Cell Biol. *38*, 1496–1509.

Sitwala, K.V., Dandekar, M.N., and Hess, J.L. (2008). HOX proteins and leukemia. Int. J. Clin. Exp. Pathol. *1*, 461–474.

Slany, R.K., Lavau, C., and Cleary, M.L. (1998). The oncogenic capacity of HRX-ENL requires the transcriptional transactivation activity of ENL and the DNA binding motifs of HRX. Mol. Cell. Biol. *18*, 122–129.

Smith, L.L., Yeung, J., Zeisig, B.B., Popov, N., Huijbers, I., Barnes, J., Wilson, A.J., Taskesen, E., Delwel, R., Gil, J., et al. (2011). Functional crosstalk between Bmi1 and MLL/Hoxa9 axis in establishment of normal hematopoietic and leukemic stem cells. Cell Stem Cell *8*, 649–662.

Somervaille, T.C., Matheny, C.J., Spencer, G.J., Iwasaki, M., Rinn, J.L., Witten, D.M., Chang, H.Y., Shurtleff, S.A., Downing, J.R., and Cleary, M.L. (2009). Hierarchical maintenance of MLL myeloid leukemia stem cells employs a transcriptional program shared with embryonic rather than adult stem cells. Cell Stem Cell *4*, 129–140.

Stelzl, U., Worm, U., Lalowski, M., Haenig, C., Brembeck, F.H., Goehler, H., Stroedicke, M., Zenkner, M., Schoenherr, A., Koeppen, S., et al. (2005). A human protein-protein interaction network: a resource for annotating the proteome. Cell *122*, 957–968.

Suzuki, M., Mizutani-Koseki, Y., Fujimura, Y., Miyagishima, H., Kaneko, T., Takada, Y., Akasaka, T., Tanzawa, H., Takihara, Y., Nakano, M., et al. (2002). Involvement of the Polycomb-group gene Ring1B in the specification of the anterior-posterior axis in mice. Development *129*, 4171–4183.

Tan, J., Muntean, A.G., and Hess, J.L. (2010). PAFc, a key player in MLL-rearranged leukemogenesis. Oncotarget *1*, 461–465.

van der Stoop, P., Boutsma, E.A., Hulsman, D., Noback, S., Heimerikx, M., Kerkhoven, R.M., Voncken, J.W., Wessels, L.F., and van Lohuizen, M. (2008). Ubiquitin E3 ligase Ring1b/Rnf2 of polycomb repressive complex 1 contributes to stable maintenance of mouse embryonic stem cells. PLoS One *3*, e2235.

Voncken, J.W., Roelen, B.A., Roefs, M., de Vries, S., Verhoeven, E., Marino, S., Deschamps, J., and van Lohuizen, M. (2003). Rnf2 (Ring1b) deficiency causes gastrulation arrest and cell cycle inhibition. Proc. Natl. Acad. Sci. USA *100*, 2468–2473.

Voss, A.K., and Thomas, T. (2009). MYST family histone acetyltransferases take center stage in stem cells and development. Bioessays *31*, 1050–1061.

Wang, J., Iwasaki, H., Krivtsov, A., Febbo, P.G., Thorner, A.R., Ernst, P., Anastasiadou, E., Kutok, J.L., Kogan, S.C., Zinkel, S.S., et al. (2005). Conditional MLL-CBP targets GMP and models therapy-related myeloproliferative disease. EMBO J. *24*, 368–381.

Whitcomb, S.J., Basu, A., Allis, C.D., and Bernstein, E. (2007). Polycomb Group proteins: an evolutionary perspective. Trends Genet. *23*, 494–502.

Yokoyama, A., and Cleary, M.L. (2008). Menin critically links MLL proteins with LEDGF on cancer-associated target genes. Cancer Cell *14*, 36–46.

Yokoyama, A., Lin, M., Naresh, A., Kitabayashi, I., and Cleary, M.L. (2010). A higher-order complex containing AF4 and ENL family proteins with P-TEFb facilitates oncogenic and physiologic MLL-dependent transcription. Cancer Cell *17*, 198–212.